An Interaction Network of RNA-Binding Proteins Involved in *Drosophila* Oogenesis

Authors

Prashali Bansal, Johannes Madlung, Kristina Schaaf, Boris Macek, and Fulvia Bono

Correspondence

f.bono@exeter.ac.uk

In Brief

The interaction network of six RBPs involved in *Drosophila* oogenesis has been determined using both label-free and dimethyl labeling MS-based proteomics. These RBPs have overlapping functions in *Drosophila* development. The results reported 26 novel associations validated *in vitro*, including interactions with splicing factors and translational regulators, suggesting a mechanism for how RBPs may regulate maternal transcripts during oogenesis. Given the evolutionary conservation of the selected RBPs, the study provides the foundation for future functional and structural studies across systems.

Graphical Abstract

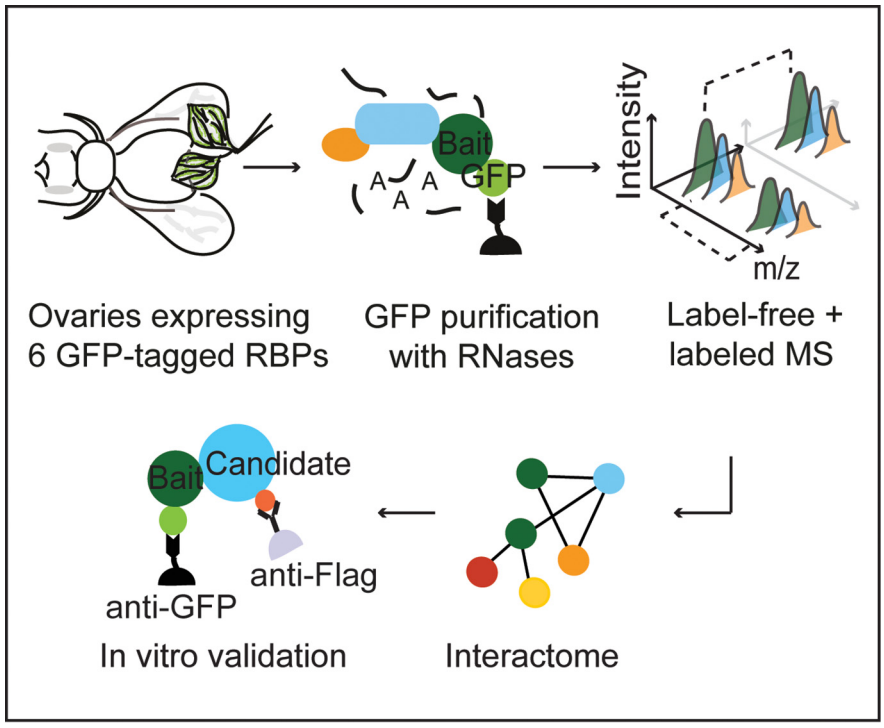

Highlights

- Label-free and dimethyl labeling MS analysis of 6 RBPs from *Drosophila* ovaries.
- Functionally related RBPs show overlapping proteomes.
- Selective co-purification of splicing factors and translational regulators.
- Validation of 26 novel interactions by co-immunoprecipitation.

Bansal et al., 2020, Mol Cell Proteomics *19(9),* 1485–1502

https://doi.org/10.1074/mcp.RA119.001912

⌘ Author's Choice

An Interaction Network of RNA-Binding Proteins Involved in *Drosophila* Oogenesis

Prashali Bansal[1,2], Johannes Madlung[3], Kristina Schaaf[2], Boris Macek[3], and Fulvia Bono[1,2,*]

During *Drosophila* oogenesis, the localization and translational regulation of maternal transcripts relies on RNA-binding proteins (RBPs). Many of these RBPs localize several mRNAs and may have additional direct interaction partners to regulate their functions. Using immunoprecipitation from whole *Drosophila* ovaries coupled to mass spectrometry, we examined protein-protein associations of 6 GFP-tagged RBPs expressed at physiological levels. Analysis of the interaction network and further validation in human cells allowed us to identify 26 previously unknown associations, besides recovering several well characterized interactions. We identified interactions between RBPs and several splicing factors, providing links between nuclear and cytoplasmic events of mRNA regulation. Additionally, components of the translational and RNA decay machineries were selectively co-purified with some baits, suggesting a mechanism for how RBPs may regulate maternal transcripts. Given the evolutionary conservation of the studied RBPs, the interaction network presented here provides the foundation for future functional and structural studies of mRNA localization across metazoans.

The post-transcriptional regulation of gene expression requires several *trans*-acting factors that regulate the life cycle of an mRNA (1). Many of these factors are RNA-binding proteins (RBPs) that interact with the maturing mRNAs to form functional messenger ribonucleoprotein complexes (mRNPs), interconnecting various steps of RNA metabolism, thereby controlling gene expression (1–3). In *Drosophila* oogenesis, mRNPs are first assembled in the nurse cell nucleus, providing a platform for the formation of larger dynamic assemblies in the cytoplasm, regulating mRNA transport, silencing and localized translation. Several RBPs have been identified and extensively studied in *Drosophila* development. Some of the well characterized and evolutionary conserved examples include the double-stranded-RNA-binding protein (dsRBP) Staufen (Stau) (4–11), the DEAD-box helicases Vasa (Vas) (12–20) and eIF4AIII (21–25), the CCHC-type zinc finger protein Nanos (Nos) (26–30) and the heterogeneous nuclear ribonucleoproteins (hnRNPs) Hrp48 and Glorund (Glo) (31–33). Binding of these proteins is essential for the proper expression of four key maternal transcripts: *bicoid (bcd)*, *oskar (osk), gurken (grk),* and *nanos (nos)* that are critical to define the future embryonic axes.

During *Drosophila* oogenesis, the anterior-posterior axis is established through the localization of *bcd* to the anterior pole and localization of *osk* and *nos* to the posterior pole of the oocyte. Accumulation of *grk* at the antero-dorsal corner determines the dorso-ventral axis of the embryo. The posterior targeting of *osk* requires several RBPs including Stau, eIF4AIII, Hrp48, Glo and Vas (4, 25, 34–38). Once localized, translation of *osk* initiates the assembly of the pole plasm by anchoring Vas to the posterior of the oocyte, a critical step in the formation of germ cells (39–41). This also results in posterior localization and activation of *nos*, essential for the embryonic abdominal patterning (42). Remarkably, many components of the *osk* mRNP regulate multiple transcripts. For example, Stau is also essential for the anterior accumulation of *bcd* mRNA in the eggs (43, 44). Hrp48, Glo and Vas regulate the localization and translation of both *osk* and *grk* transcripts (35–38, 40, 45–47). Glo also represses nonlocalized *nos* in the oocytes (48), whereas Vas promotes *nos* translation in the embryos (49).

In addition to their functions in establishing oocyte polarity, these RBPs have various other roles during *Drosophila* oogenesis. For example, Hrp48 and Glo are required in nurse cells for the regulation of chromosome organization (38, 47). They have also been implicated as regulators of alternative splicing, like their mammalian homologs (38, 50–52). During early oogenesis, both Vas and Nos are involved in the maintenance of germline stem cells, in oocyte differentiation, and other aspects of oocyte development (26, 35, 53–56). In embryos, Nos functions in germline development (53, 57–61) and further promotes the inclusion of germline cells in the developing ovary (53, 62). In addition to oogenic processes, Nos and Stau are also involved in the development of the *Drosophila* nervous system (63, 64).

From the [1]Living Systems Institute, University of Exeter, Exeter, UK; [2]Max Planck Institute for Developmental Biology, Tübingen, Germany; [3]Proteome Center Tübingen, Interfaculty Institute for Cell Biology, Eberhard Karls University, Tübingen, Germany

This article contains supplemental data.

*For correspondence: Fulvia Bono, f.bono@exeter.ac.uk.

DOI 10.1074/mcp.RA119.001912

Many RBPs in *Drosophila* oogenesis have overlapping functions that are likely differentially regulated. Little is known about this regulation and it may involve several as yet unidentified mRNP components. To comprehensively identify RBP interactors, we carried out a systematic *in vivo* purification screen of GFP-tagged RBPs coupled with MS. We employed both labeled and label-free MS methods and identified several proteins significantly enriched with the purified RBPs. The interactomes of the individual RBPs were largely independent with some overlap. Our screen identified several previously unknown interactions, many of which we validated *in vitro*. This work presents an extended interaction network of RBPs in *Drosophila*, offering a new reference point for future functional and structural studies of mRNA localization.

EXPERIMENTAL PROCEDURES

Cloning and DNA Constructs—For cloning purposes, total RNA was extracted from WT ovaries using the TRI-Reagent (Sigma), according to the manufacturer's instructions. RNA was reverse transcribed using Moloney Murine Leukemia Virus (M-MuLV) reverse transcriptase (Thermo Fisher Scientific), in the presence of oligo $(dT)_{15}$ primers. To express proteins in human HEK293 cells, genes of interest were amplified from *Drosophila* cDNA, or in some cases from the Drosophila Genomics Resource Center (DGRC) clones, using standard PCR conditions. Accession numbers of all the genes cloned are provided in supplemental Table S1. Fragments were cloned into mammalian expression vectors based on pEGFP-C1 (CLONTECH), bearing an N-terminal EGFP tag or modified to contain either HA or HA-Flag tags (provided by Elisa Izaurralde, MPI Tübingen). Full-length cDNAs were cloned, except for the protein Nucampholin (Ncm), where a sequence encoding amino acids 359-664 was amplified. The boundaries were designed based on the MIF4G domain of the human ortholog CWC22, which has been shown to bind eIF4AIII (65). To serve as a control, either MBP or EGFP alone was used.

Drosophila Stocks—All flies were kept at room temperature on standard *Drosophila* medium. Oregon R flies were used as WT. Fosmid lines expressing GFP-tagged proteins (66) were purchased from the Vienna Drosophila Resource Center (VDRC 318283, 318719, 318195, 318157, 318898, 318766). To generate the control fly-line expressing the tag only, the tag sequence was cloned in a modified pUAST-attB vector (67) (without UAS sites or SV40 poly(A) signal), downstream of a moderately expressing *exu* promoter using KpnI and BamHI sites. The purified vector was injected into embryos from a recombinant stock with a genotype y[1] M{vas-int.Dm} ZH-2A w[*]; PBac{y[+]-attP-3B}VK00033 (BDSC 24871). Transgenic flies were identified in the F1 generation by the presence of red eyes (dsRed) and a stable fly line was established.

Cell Culture and co-IP from HEK Cells—Human HEK293 cells were grown at 37 °C in the presence of 5% CO_2 in standard Dulbecco's Modified Eagle Medium, supplemented with 10% heat-inactivated fetal bovine serum, Glutamine and Penicillin-Streptomycin solution.

For co-immunoprecipitations (co-IP), transfections were carried out in six-well plates with Lipofectamine 3000 (Invitrogen) according to the manufacturer's recommendations. Typically, 5 μg of DNA was transfected in each well and the ratio of two plasmids was adjusted based on their expression levels. If required, a third empty plasmid with HA tag was supplemented, to reach a total amount of 5 μg. Cells were collected 2 days after transfection and washed with PBS before lysis. Cells were lysed for 15 min on ice in a buffer containing 50 mM Tris-HCl pH 7.5 at 4 °C, 100 mM NaCl, 250 mM Sucrose, 0.1% Nonidet P-40, 1 mM DTT, supplemented with protease inhibitors (cOmplete™, EDTA-free Protease inhibitor mixture, Roche). For efficient lysis, cells were mechanically sheared by passing them through a needle (Sterican 21G 7/8" Ø 0.8X22mm) several times. Cell lysates were cleared at 16,000 × *g* for 15 min at 4 °C and supernatants were incubated with 5 μl/ml of RNase A/T1 (Thermo Fisher Scientific) for 30 min at 4 °C. After clearing the lysate again at 16,000 × *g* for 15 min, 12-20 μl of GFP-TRAP MA beads (Chromotek) were added to the supernatant and the mixtures were rotated for 1 h at 4 °C. For Flag pull-downs, 1.8 μg of monoclonal anti-Flag antibody (Sigma #F1804) was added to the supernatant, after the RNase treatment. After 1 h at 4 °C in rotation, 20 μl of GammaBind Plus Sepharose beads (GE Healthcare) were added, and the mixtures were rotated for an additional hour at 4 °C. Beads were washed with lysis buffer and proteins were eluted in sample buffer by boiling at 95 °C for 10 min.

Immunoprecipitation from Drosophila Ovaries—Ovaries from well-fed flies were dissected in PBS and stored at −80 °C. For immunoprecipitation, frozen ovaries were thawed on ice in lysis buffer (50 mM Tris-HCl pH 7.5 at 4 °C, 100 mM NaCl, 250 mM Sucrose, 0.1% Nonidet P-40 and 1 mM DTT) and pooled together in required numbers (see supplemental Table S2). Ovaries were homogenized with a glass pestle in a tissue homogenizer in lysis buffer (320 μl/40 flies) supplemented with protease inhibitors (cOmplete™, EDTA-free Protease inhibitor mixture, Roche). Lysates were cleared by centrifugation at 21,000 × *g* for 20 min at 4 °C and 5 μl/ml of RNase A/T1 (Thermo Fisher Scientific) was added to the supernatants. After incubation at 4 °C for 30 min, lysates were cleared again and 30–60 μl of GFP-TRAP MA beads (Chromotek, Planegg-Martinsried, Germany) were added. The mixtures were incubated for 1 h at 4 °C in rotation. Beads were washed with lysis buffer and proteins were eluted as described above.

Western Blotting and Detection—Eluates were separated on 10% polyacrylamide gels and transferred to a nitrocellulose membrane. Membranes were blocked in PBS containing 5% milk powder and 0.1% Tween-20. HA-tagged, HA-Flag-tagged and GFP-tagged proteins were detected using HRP-conjugated monoclonal anti-HA (1:5000, BioLegend #901501) or polyclonal anti-GFP antibodies (1:2000, Thermo Fisher Scientific #A11122) respectively. Blots were developed with ECL (GE Healthcare) reagents, as recommended by the manufacturer, and imaged using an Amersham Pharmacia Biotech Imager 600 (GE Healthcare). The raw immunoblots are shown in supplemental data S6.

Experimental Design and Statistical Rationale—For analysis of proteins interacting with each tagged RBP, both label-free and dimethyl labeling MS experiments were performed and raw data were processed by the MaxQuant software as described below. Proteome data comprised a total of 21 raw files (3 biological replicates from each sample) for label-free MS and 2 raw files (2 biological replicates from each sample) for dimethyl labeling MS. Tag alone was used as a negative control for both analyses.

Mass Spectrometry Measurements—For proteome measurements, eluates were separated on a NuPAGE Bis-Tris precast 4-12% gradient gel (Invitrogen). Samples were run ~2 cm into the gel and bands were visualized with a 0.1% Colloidal Coomassie Blue stain (Serva, Heidelberg, Germany). Proteins were digested in-gel using trypsin. Peptides were desalted and purified on C18 StageTips (68). LC–MS analysis was carried out on a nanoLC (Easy-nLC 1200, Thermo Fisher Scientific) coupled to a Q Exactive HF mass spectrometer (Thermo Fisher Scientific) through a nanoelectrospray ion source (Thermo Fisher Scientific), as described previously (69). In brief, peptides were eluted using a segmented gradient of 10%–50% HPLC solvent B (80% ACN in 0.1% formic acid) at a flow rate of 200

nL/min over 46 min MS data acquisition was conducted in the positive ion mode. The mass spectrometer was operated in a data-dependent mode, switching automatically between one full scan and subsequent MS/MS scans of the 12 most abundant peaks selected with an isolation window of 1.4 *m/z* (mass/charge ratio). Full-scan MS spectra were acquired in a mass range from 300 to 1650 *m/z* at a target value of 3×10^6 charges with the maximum injection time of 25 ms and a resolution of 60,000 (defined at *m/z* 200). The higher-energy collisional dissociation MS/MS spectra were recorded with the maximum injection time of 45 ms at a target value of 1×10^5 and a resolution of 30,000 (defined at *m/z* 200). The normalized collision energy was set to 27%, and the intensity threshold was kept at 1×10^5. The masses of sequenced precursor ions were dynamically excluded from MS/MS fragmentation for 30 s. Ions with single, unassigned, or six and higher charge states were excluded from fragmentation selection.

For dimethylation labeling, after tryptic in-gel digestion, derived peptides were loaded on C18 StageTips and labeled as described (70). Measurements were done the same way as for the unlabeled samples.

Data Processing and Analysis—For label-free MS, raw data files were processed using the MaxQuant software suite v.1.6.0.1 (71) at default settings. Using the Andromeda search engine (71) integrated in the software, the spectra were searched against the UniProt *D. melanogaster* (taxonomy ID 7227) complete proteome database (11/07/2017; 23300 protein entries; https://www.uniprot.org/), a database comprising a sequence of the tag alone and a file containing 245 common contaminants. In the database search, Trypsin was defined as a cleaving enzyme and up to two missed cleavages were allowed. Carbamidomethylation (Cys) was set as a fixed modification, whereas oxidation (Met) and acetylation (protein N termini) were set as variable modifications. The mass tolerances for precursor and fragment ions were set to default values of 20 ppm and 0.5 Da, respectively. The MaxLFQ algorithm was activated and the minimum number of peptide-ratio count was set to 1 (73). All peptide and protein identifications were filtered using a target-decoy approach with a false discovery rate (FDR) set to 0.01 at peptide and protein level (72). A valid protein identification required at least one peptide with a posterior error probability (PEP) value of 0.01 or smaller. To transfer peptide identifications to unidentified or unsequenced peptides between samples for quantification, the "matching between runs" option was selected, with a match time window of 0.7 min and an alignment time window of 20 min. Matching was performed only between replicates by controlling the fraction numbers. The same parameters were used to process the raw data from the experiments applying dimethyl labeling, except for the following: MaxQuant software suite v. 1.5.2.8 was used; MS spectra were searched against a reference *D. melanogaster* proteome obtained from Uniprot (16/10/2015; 23334 protein entries; https://www.uniprot.org/); dimethylation on peptide N termini and lysine residues was defined as light (+28.03 Da), intermediate (+32.06 Da), and heavy (+36.08 Da); re-quantification was enabled; no matching between runs was applied; quantitation of labeled peptides required at least two ratio counts. Experiments were carried out in biological duplicates (supplemental Table S2) and labels were swapped to correct for errors in the labeling procedures.

Bioinformatics analysis of the label-free MS data were done using Perseus v. 1.6.5.0 (73) (supplemental data S2). Protein identifications were filtered for potential contaminants, for proteins identified only by modified peptides and for peptides derived from the reversed sequence of the decoy database. Protein intensity values were logarithmized (Log2) and replicates for each bait were grouped together. For identification of protein interactions, the data were analyzed in a pairwise fashion *i.e.* each individual bait group against the control group. Proteins were filtered based on the identification of minimum three valid values in at least one replicate group. As the data followed a normal distribution, the missing values were imputed (using 0.3 standard deviations width reduction and 1.8 standard deviations downshift) enabling statistical analysis. Both-sided Welch's *t* test was used with an s_0 value of 2, to control the artificial within-group variance. For each test, to filter the rows, a requirement of at least 2 valid values in the bait group was set, further controlling the effects of imputation. A 5-10% FDR cutoff (permutation-based; number of randomizations: 250 without preserving groupings) was set to determine significantly enriched proteins. The same pipeline was employed for all the pairwise analyses.

For analyzing dimethyl labeling MS data, the ratio for each sample was normalized to the median of the distribution through MaxQuant (74), to correct for mixing errors. Normalized ratios were Log2-transformed and ratios from duplicates were plotted against each other. Statistically significant differences in abundance were determined by applying an arbitrary ratio threshold of 1 in Log2 scale (2-fold).

All the scatter plots and the volcano plots were generated using GraphPad Prism v. 7.0.0. For creating networks or subnetworks, Cytoscape v. 3.7.1 (75) was used. To integrate IP-MS data with literature, information from databases like String v. 11.0 (76) and FlyBase (77) were used. From String, only experimental data with medium confidence range was considered. Physical interaction data from FlyBase (77) were extracted for each protein individually. Node size calculation: for dimethyl labeling data, average of the enrichment ratios of duplicates was calculated for each protein. If a protein was found to be associated with more than one bait or identified in both label-free and labeled MS data, the highest fold change value was considered, irrespective of the experiment type. In cases where several nodes were combined into one, the highest value among the respective individual components was considered. Fig. 4 was created using Gephi v. 0.9.2 (78). Modules were detected with an algorithm described in (79), with randomization on, using edge weights and a resolution of 0.5. Force-field-based clustering was performed using the Force Atlas 2 Plugin. Baits were re-positioned manually for clarity.

For GO term analysis, the DAVID (**D**atabase for **A**nnotation, **V**isualization and **I**ntegrated **D**iscovery) v. 6.8 functional annotation tool was used (80, 81), which adopts Fisher's Exact test to measure the gene-enrichment in annotation terms. The following parameters were used: background: *Drosophila* genome; count threshold (minimum number of genes for that term) of 2; maximum ease score (modified Fisher's Exact P-value) of 0.01. To reduce redundancy in the GO terms, the DAVID output was fed into REVIGO (**Re**duce + **Visualize** **G**ene **O**ntology) (82) and *p*-values were used to select and cluster GO terms with a similarity score of 0.7 (medium). The *Drosophila* database was used to find the GO term sizes (supplemental data S1).

RESULTS

Tagged Proteins Recapitulate the Endogenous Localization Patterns—To purify RBP complexes from fly ovaries under native conditions, we used transgenic fly lines generated by recombineering. We used the "Tagged FlyFos TransgeneOme" resource (fTRG) (66) expressing C-terminally-tagged proteins under the regulation of their endogenous promoters. These lines carry a 40 kDa tagging cassette consisting of "2XTY1-sGFP-V5-preTEV-BLRP-3XFLAG" that can be used for both *in vivo* visualization and affinity purification. From the fTRG library, we selected six RBPs for IP-MS, eIF4AIII, Glo, Hrp48, Nos, Stau and Vas. To serve as a control, we

generated a transgenic line expressing the tag alone (hereafter referred to as GFP), under the promoter of a moderately expressing gene (*exu*). To ensure that the RBP fusions are functional *in vivo*, we checked their localization patterns at different stages of oogenesis. All the proteins were found to be localized as expected (supplemental Fig. S1*A*–S1*I*). In agreement with previous work, we observed eIF4AIII-GFP in the nucleus of the nurse cells and localized to the posterior of the oocyte at stage 5 of oogenesis (supplemental Fig. S1*C*; 25). eIF4AIII was also reported to enrich weakly at the posterior of the oocyte at stage 9 (25), which we could not detect in our samples. We could detect Glo-GFP in the nucleus of the nurse cells, the oocyte and follicle cells, consistent with the antibody-based localization of endogenous Glo (supplemental Fig. S1*D*; 48). Hrp48-GFP was present in the cytoplasm of the nurse cells and localized to the posterior of the oocytes at stage 9, similar to Vas-GFP (supplemental Fig. S1*E*, S1*G*; 46, 83). We also observed the nuage localization of GFP-tagged Vas at early stages, consistent with previous studies (supplemental Fig. S1*G*; 83). At stage 8, Stau-GFP was concentrated at the anterior of the oocyte, whereas stage-9 egg chambers showed a strong posterior enrichment (supplemental Fig. S1*F*; 4). In the nurse cells of stage-10 egg chambers, Nos-GFP showed a strong uniform GFP expression, as also observed by Wang and colleagues (62). In addition to the localization patterns of the tagged RBPs, we also checked their ability to rescue the effects of mutations that cause either lethality or sterility, as summarized in supplemental Fig. S1*J*. Although only 3 out of 6 transgenes assayed were able to fully substitute for the endogenous copy, their localization in the endogenous patterns suggests that their interactions driving localization during oogenesis have been maintained.

Label-Free MS Combined with Statistical Analysis Recovers Known Associations—For IP, we lysed whole ovaries in mild conditions of salt and detergent, and purified the complexes using the GFP-TRAP system (Chromotek) (Fig. 1*A*). An IP from flies expressing GFP alone was used as a negative control to identify proteins binding nonspecifically to the tag. Because we were interested in identifying RNA-independent protein-protein interactions, the experiments were carried out in the presence of RNases. As the transgenes are regulated by their endogenous promoters, they had varying levels of expression, as observed by Western blotting (Fig. 1*B*). To compensate for this variability in the IP-MS analysis, we adjusted the number of flies dissected for each transgene (supplemental Table S2).

All the samples were prepared in biological triplicates and the resulting spectra were searched against the *Drosophila melanogaster* proteome database (Fig. 1*A*, supplemental Fig. S2*A*). For confident identification of proteins and accurate intensity-based Label-Free Quantification (LFQ), we processed the raw data using the MaxLFQ module of the MaxQuant software (74, 84). Additionally, we activated the "matching between runs" algorithm to quantify unidentified or unsequenced peptides in the samples, by transferring peptide identifications among replicates. The global analysis of the proteomes resulted in the identification of 15,005 peptides mapping to 1878 protein groups, at a FDR of 1% at the peptide and protein level. Of these, 1841 unique protein groups were quantified in at least one of the 21 samples, which account for 87.5% of the total ovary proteome of *Drosophila* (85). The average correlation within replicates ranged from 0.71 (Glo) to 0.92 (Hrp48), suggesting overall good reproducibility of the data (Fig. 1*C*). In addition, the visualization of LFQ intensities of all the samples as a heat map demonstrates that all the baits were consistently enriched (supplemental Fig. S2*C*). The replicate profiles looked largely similar, with only minor differences. However, the number of proteins quantified with each bait varied highly, as marked by the absence of information in the heat map (supplemental Fig. S2*C*).

For statistical analysis, we considered only those proteins that were quantified in all three replicates of a given sample. To identify significantly enriched proteins, we employed the Welch's *t* test (with 5–10% FDR cutoff), post-imputation, on each bait-control matrix. The results are presented as volcano plots in Fig. 2*A*. All the baits were highly enriched and we observed a minimal background, indicating the high specificity of the purifications. For the baits eIF4AIII-, Stau- and Glo-GFP, where fewer proteins were reproducibly quantified, we considered statistical significance up to 10% FDR. The low number of detections for these proteins may be because of the loss of interactions on RNase treatment.

For all the baits, we found several known interactants to be reproducibly enriched over control, mostly with statistical significance (Fig. 2*A*, supplemental Data S5). For example, we co-purified all the other core components of the Exon Junction Complex (EJC) with eIF4AIII-GFP (25) and the NOT proteins with Nos-GFP (86, 87). We also detected known partners of Vas, involved in both pole plasm assembly in the oocyte (Oskar (Osk); Gustavus (Gus); Fat facets (Faf); F-box synaptic protein (Fsn); Fmr1) and production of germline piRNAs in the nuage (Tejas (Tej); Spindle-E (SpnE); Kumo (Qin); Tapas), with high confidence (88). Previously identified Hrp48-interacting partners such as Ovarian Tumor (Otu), Cup, PABP, Squid (Sqd) and Syncrip (Syp), involved in maternal mRNA regulation were also co-purified with the Hrp48-GFP bait (47, 89, 90). This indicates that our experimental conditions and analysis pipeline can preserve and identify true interactions. In addition, we also identified proteins that are known to be indirectly associated with Vas, such as the Cullin proteins (91) and Tudor-domain proteins Tudor (Tud) (92) and Krimper (Krimp) (93), suggesting that we not only recovered direct interactants, but whole complexes functional in distinct pathways (supplemental Fig. S3). With the Glo-GFP bait, we reproducibly identified other hnRNPs, including Hrp48 and the splicing factor Half pint

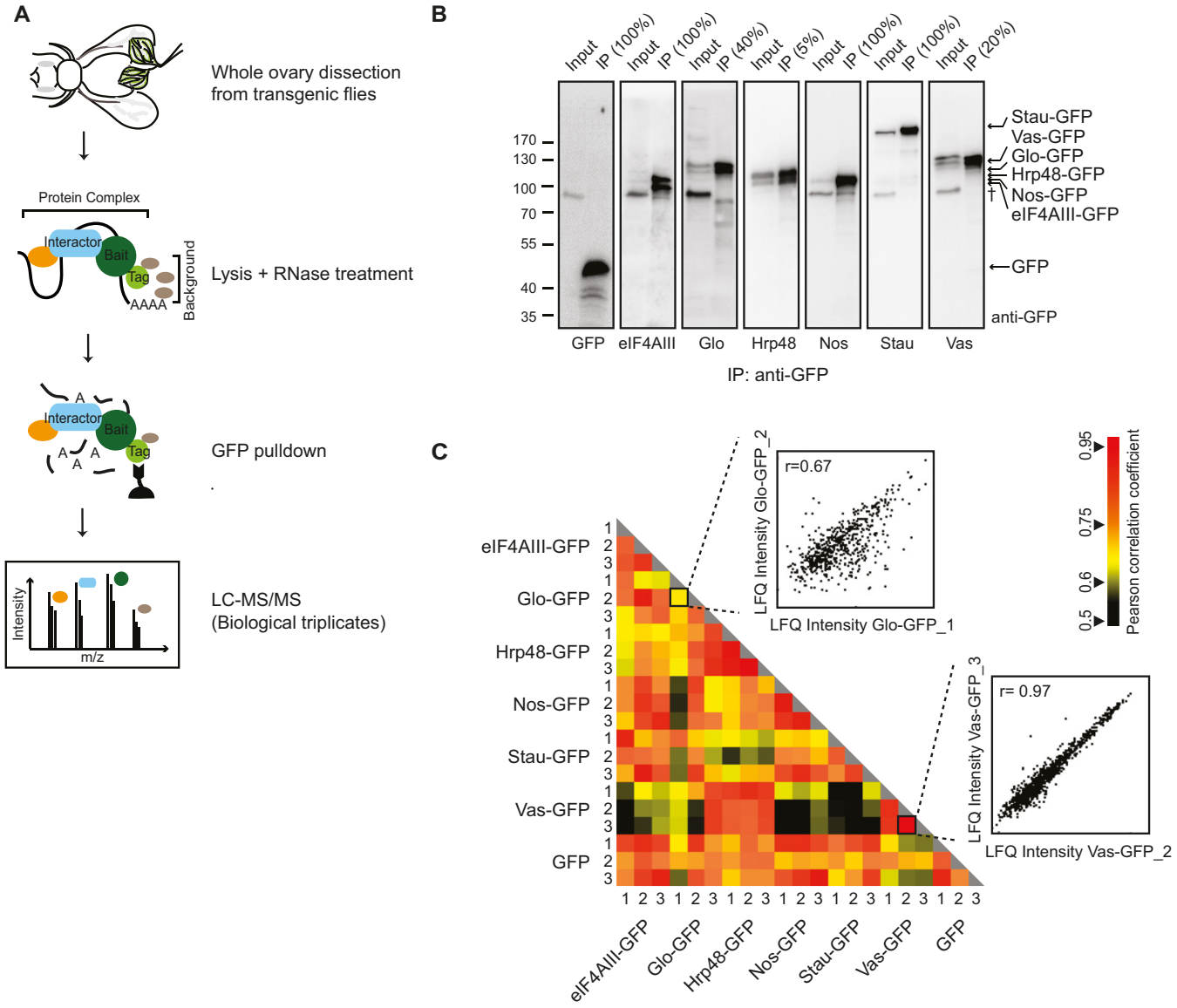

FIG. 1. **Isolation of bait-associated complexes using IP-MS.** *A*, Schematic representation of the IP-MS workflow. Whole ovaries were isolated from transgenic flies expressing GFP-tagged proteins (baits) and complexes were purified using an anti-GFP nanobody coupled to magnetic beads. Lysates were treated with RNases before immunoprecipitation. IP from a transgenic line expressing GFP served as a control. Eluates were analyzed by LC–MS/MS. *B*, Presence of tagged baits in the immunoprecipitates was checked by Western blot, probed with anti-GFP. Inputs and eluates were loaded in different amounts for efficient visualization. Input of the total lysate: 2.1% for GFP, eIF4AIII, Nos; 4.2% for Glo, Vas, Stau and 1.2% for Hrp48. Loading of the respective eluates is highlighted on the top of each lane. † is an unspecific interaction detected by the antibody. *C*, Heat map representation of the matrix of Pearson correlation coefficient calculated between LFQ intensities of the complexes, each isolated in triplicate. The zoomed plots show the highest and lowest coefficient values (r) among the replicates.

(Hfp), consistent with previous reports (38, 94). Similarly, we could also recover an interaction of Stau-GFP with the spliceosomal protein SmB (95). However, the enrichment was not significant for these proteins, suggesting weak or transient interactions.

Quantitative Analysis Complements the Label-Free MS Data—To detect fold changes in protein abundances with high precision, we used dimethyl labeling MS. This approach is advantageous for *Drosophila*, where metabolic isotopic labeling is still challenging. To confirm the results of our label-free analysis, we carried out dimethyl labeling MS for the Hrp48- and Vas-GFP samples. We chose Hrp48 and Vas as these proteins express well and they are involved in the localization and translational regulation of both *osk* and *grk* during *Drosophila* oogenesis (35–37, 40, 45–47). We carried out the experiments in duplicates and purified the samples the same way as for label-free MS (supplemental Fig. S2*B*). After in-gel digestion, we labeled the peptides with heavy, medium, or

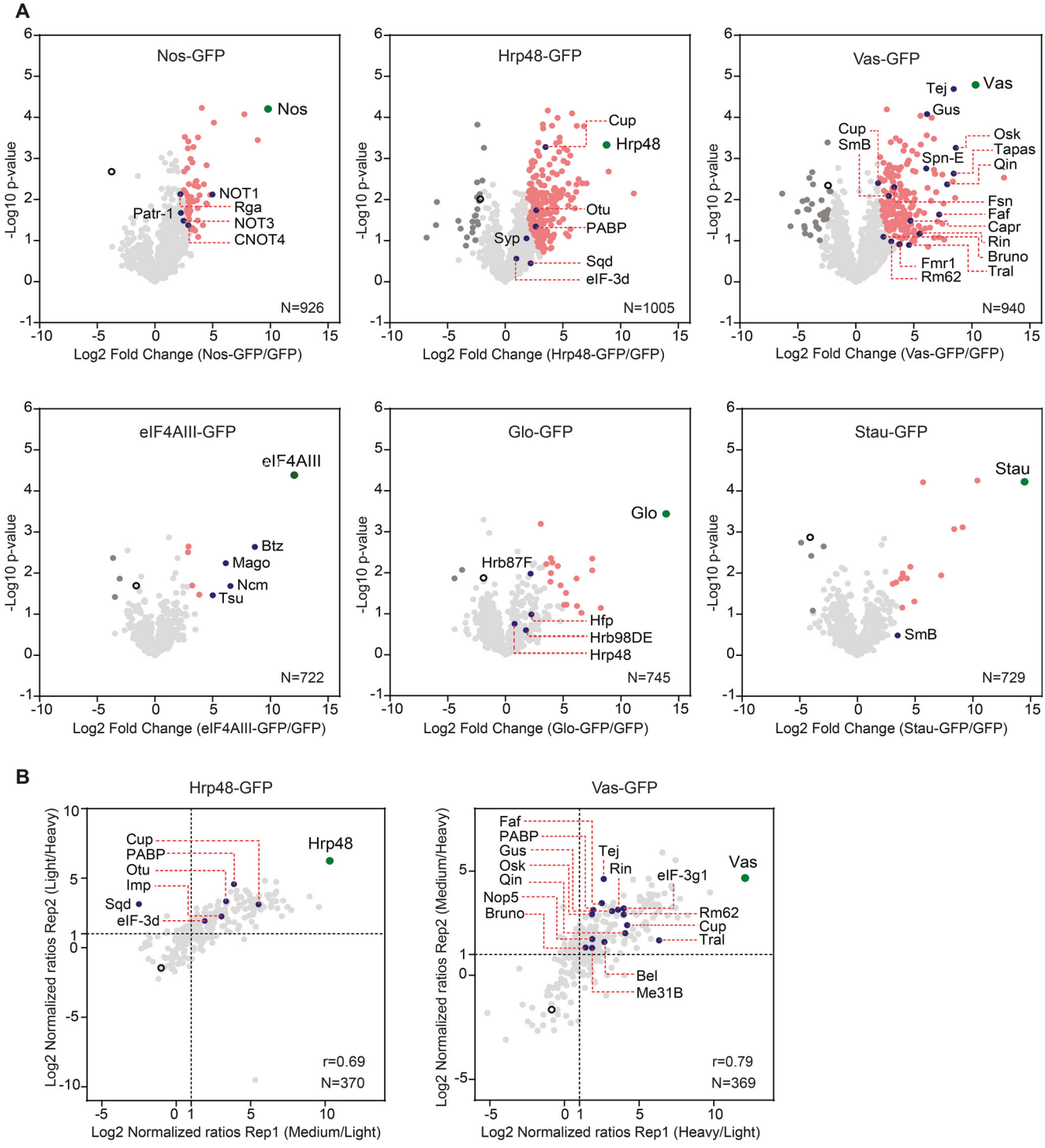

FIG. 2. **Interactants, including known and new partners, were significantly enriched.** *A*, Volcano plots of proteins identified to be associated with each bait in the label-free MS analysis, after filtering and data imputation. The significance of enrichment was calculated using the two-tailed Welch's *t* test, with FDR < 0.05, $s_0 = 2$ for Nos, Hrp48 and Vas, and FDR < 0.1, $s_0 = 2$ for eIF4AIII, Glo and Stau. For each bait-control pair, the resulting differences between the logarithmized means of the two groups "Log2(bait/control)" and the negative logarithmized *p* values were plotted against each other. *B*, Scatter plots of the proteins identified to be associated with Hrp48-GFP and Vas-GFP in the dimethyl labeling MS analysis. Normalized ratios (Log2) of both the replicates were plotted against each other. Dotted lines mark the proteins with more than 2-fold change over control, in each replicate. IP from GFP sample served as a control. "N" denotes the number of protein groups plotted and "r" denotes the Pearson correlation coefficient. Each identified protein is represented as a dot in light gray; each bait is highlighted in green; significantly enriched proteins are highlighted in pink; known interactants are highlighted in blue; background binders are highlighted in dark gray; empty circle represents control.

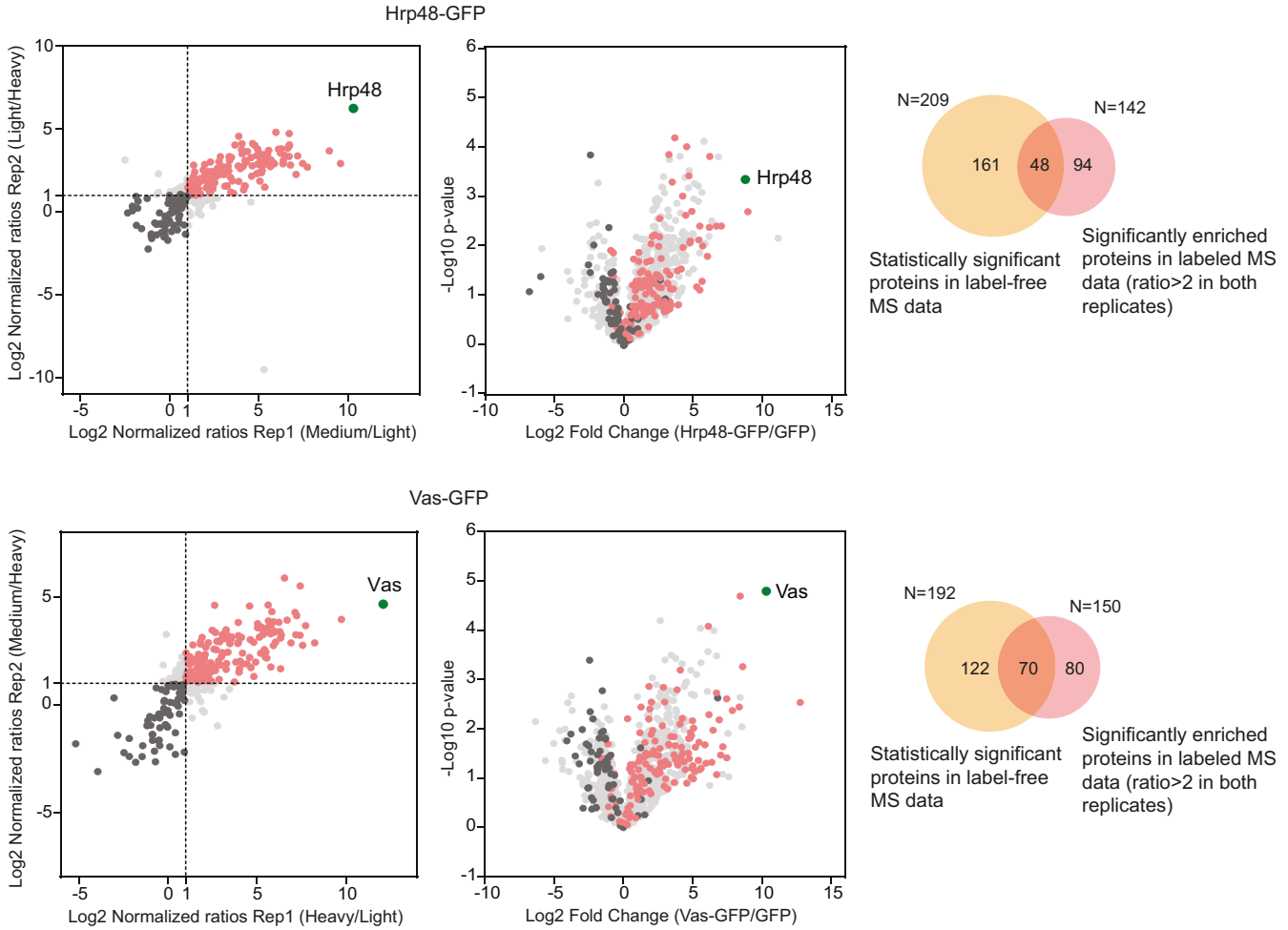

FIG. 3. **Quantitative label-based MS data support the label-free MS data.** Data from the labeled analysis (represented as scatter plots) was compared with the label-free analysis (represented as volcano plots) by overlaying the proteins identified in the respective Hrp48-GFP (top) and Vas-GFP (bottom) IP-MS samples. Venn diagrams represent the overlap between the significantly enriched interactants found in the two data sets. "N" denotes the number of proteins analyzed. In the scatter/volcano plots, each identified protein is represented as a dot in light gray; baits are highlighted in green; significantly enriched proteins are highlighted in pink; background binders are highlighted in black.

light isotopes and inverted the labels in the replicate, to minimize the variability because of the labeling procedures. As before, the raw data were processed with the MaxQuant software (74), providing confident identification of proteins (1% FDR) and normalized protein-abundance ratios. The analysis of the Vas- and Hrp48-associated proteomes resulted in the identification of 4027 peptides, mapping to 615 protein groups. The replicates showed high correlation and the abundance ratios calculated could be well duplicated. We considered as a hit those proteins that we identified with an abundance ratio of >2 in both replicates. Consistent with the label-free analysis, we found several known interactors, most of them reproducibly enriched (Fig. 2*B*). To check how the two analyses relate to each other, we mapped the proteins identified in labeled MS onto the label-free MS data. As shown in Fig. 3, the proteins that were significantly enriched in the labeled MS followed the same distribution profile and showed up to 47% overlap (for Vas) with those enriched in the label-free MS analysis. Background proteins identified in labeled MS (<2 fold in both replicates) showed a similar profile when graded on the corresponding label-free MS data (Fig. 3). To get a comprehensive view of the proteomes associated with Hrp48 and Vas, we combined the enriched proteins from both analyses.

Global Analysis of RBP Interactomes Reveals Novel Protein Interactions—To understand how the proteomes identified with each bait interact with each other, we built a composite network of all statistically significant interactants. Although each bait has interaction partners that do not interact with any of the other baits (for example, Stau interaction with RNA silencing proteins Dicer and its co-factor Loquacious (Loqs)), the network is also highly connected. In addition to the considerable overlap in the proteomes of the functionally related hnRNPs Hrp48 and Glo, we observed that Hrp48 and Vas also shared a significant number of interacting proteins (supplemental Fig. S4, supplemental Data S3). This overlap

suggests the interplay of these protein modules in the localization of transcripts during *Drosophila* development (96). To gain a systemic understanding of the network, we also added the known protein-protein associations from the String v. 11.0 (76) and FlyBase (77) databases. Next, we carried out a modularity analysis to identify highly connected communities of proteins (Fig. 4*A*, supplemental Data S4). As expected, many proteins involved in oogenesis, mRNA localization, translational regulation and germ cell formation were selectively enriched with all the baits. Additionally, proteins involved in neurogenesis and splicing were also overrepresented, consistent with the well-studied function of selected RBPs in these processes (Fig. 4*B*).

Interestingly, we observed ribosomal proteins (components of both large and small subunits) to be significantly enriched with Vas-GFP and Hrp48-GFP, but not with the other RBPs analyzed (Fig. 5, supplemental Fig. S4). Previous studies have shown the requirement of Vas in translational activation of *osk, nos* and *grk* mRNAs (35, 36, 40, 49). However, the molecular mechanism by which Vas activates translation is unclear. Studies in *Drosophila* have shown that Vas directly binds the translation initiation factor eIF5B (dIF2) to positively regulate *grk* and *mei-P26* translation and possibly other germline-specific transcripts (97–99). In addition, Vas also interacts genetically with the translation initiation factor eIF4A for efficient germ cell formation (100). However, neither eIF5B nor eIF4A were detected or enriched in our data set. Instead, other translation initiation factors involved in the formation of the pre-initiation complex, such as eIF2, eIF3 and the cap-binding complex of eIF4E-4G were selectively co-purified (Fig. 5). This is consistent with the recently reported interaction of eIF3 subunits with Vas in the *Drosophila* oocytes (56).

Hrp48 is required for the translational repression of *osk* and *grk* mRNAs (45–47). Consistent with this, we co-purified with Hrp48-GFP (in both label-free and labeled MS experiments) several P-body-components, associated with the RNA repression/decay machinery, most notably the deadenylase and decapping complexes (Fig. 6). Ribosomal proteins and translation initiation factors were also significantly enriched with the Hrp48-GFP bait, similar to Vas-GFP (Fig. 5). This includes eIF3d, which has recently been reported to interact with Hrp48 to translationally repress the *msl-2* mRNA (101).

In Vitro Validation of Protein-Protein Interactions—To validate the results of our IP-MS analysis, we co-expressed bait-candidate pairs in cultured mammalian HEK293 cells (Fig. 7). This system can be effectively used to study direct interactions of *Drosophila* proteins because it reduces the likelihood of endogenous proteins mediating indirect associations. For validation, we selected significantly enriched candidates identified in the label-free MS analysis. Additionally, we also considered functionally relevant partners, enriched with a >2 times fold change but excluded by statistical filtering. For Hrp48 and Vas, where information from differential labeling was also available, we selected candidates among the interacting proteins identified in both data sets.

Typically, we co-expressed an EGFP (referred to as GFP)-tagged bait with an HA-tagged candidate protein and used the GFP-TRAP system (Chromotek) to carry out IPs in the presence of RNases. We observed that small proteins ($<$25kDa) expressed poorly as fusions with HA or HA-Flag. In these cases, we switched the tags. Substitution with the GFP tag improved the expression of the candidate proteins in all the cases tested. To be able to validate the interactions of such small proteins, we co-expressed a GFP-tagged candidate with an HA-Flag-tagged bait and performed the IP with anti-Flag (Fig. 7*B*, 7*D*). Because Vas does not express well as an HA- or HA-Flag fusion, we could not test the interactions of small protein candidates with Vas. As negative controls, we used MBP or GFP. We also included known interactions as positive controls, wherever possible. All the tested candidates are indicated in supplemental Fig. S5.

Out of 90 protein-protein interactions assayed, we could confirm 32 interactions (35%), of which 26 were found to be novel (summarized in Fig. 7*J*). Similar studies from *Drosophila* ovaries or embryos have shown a validation rate of $<$25% (56, 102). All positive interactions were confirmed at least 3 times, in independent experiments. In addition, we were also able to validate some of the interactions by reciprocal IP, as shown in Fig. 7*C*. To further confirm that our MS analysis pipeline effectively separated background binders from true interactants, we also tested Nucleophosmin (Nph), which was depleted in all IP-MS data sets. We could not detect interactions of Nph with any of the 4 baits tested *in vitro* (data not shown), in line with the MS data. Additionally, we also tested Sqd that has been reported to interact with Hrp48 in an RNA-dependent manner (47). The negative results further confirm that our experimental conditions effectively disrupted RNA-mediated associations. However, we cannot exclude the possibility that some interactions could be indirect and mediated by human factors or residual RNA impurities. Also, many interactions that were determined to be significant in the MS data analysis could not be validated in our *in vitro* assay. This could be because of the lack of post-translational modifications, protein misfolding, low affinity or indirect interactions. To visualize the co-IP results, we integrated the validated interactions with the IP-MS data (both labeled and label-free) and information from the literature to create a subnetwork (supplemental Fig. S6). As the majority of the validated interactants are known regulators of maternal mRNAs, this subnetwork highlights an extended interaction network potentially involved in the regulation of mRNAs during *Drosophila* oocyte development.

DISCUSSION

This study presents a proteome interaction network of six RBPs (eIF4AIII, Hrp48, Glo, Nos, Stau and Vas) required for the localization of maternal mRNAs in *Drosophila*. To

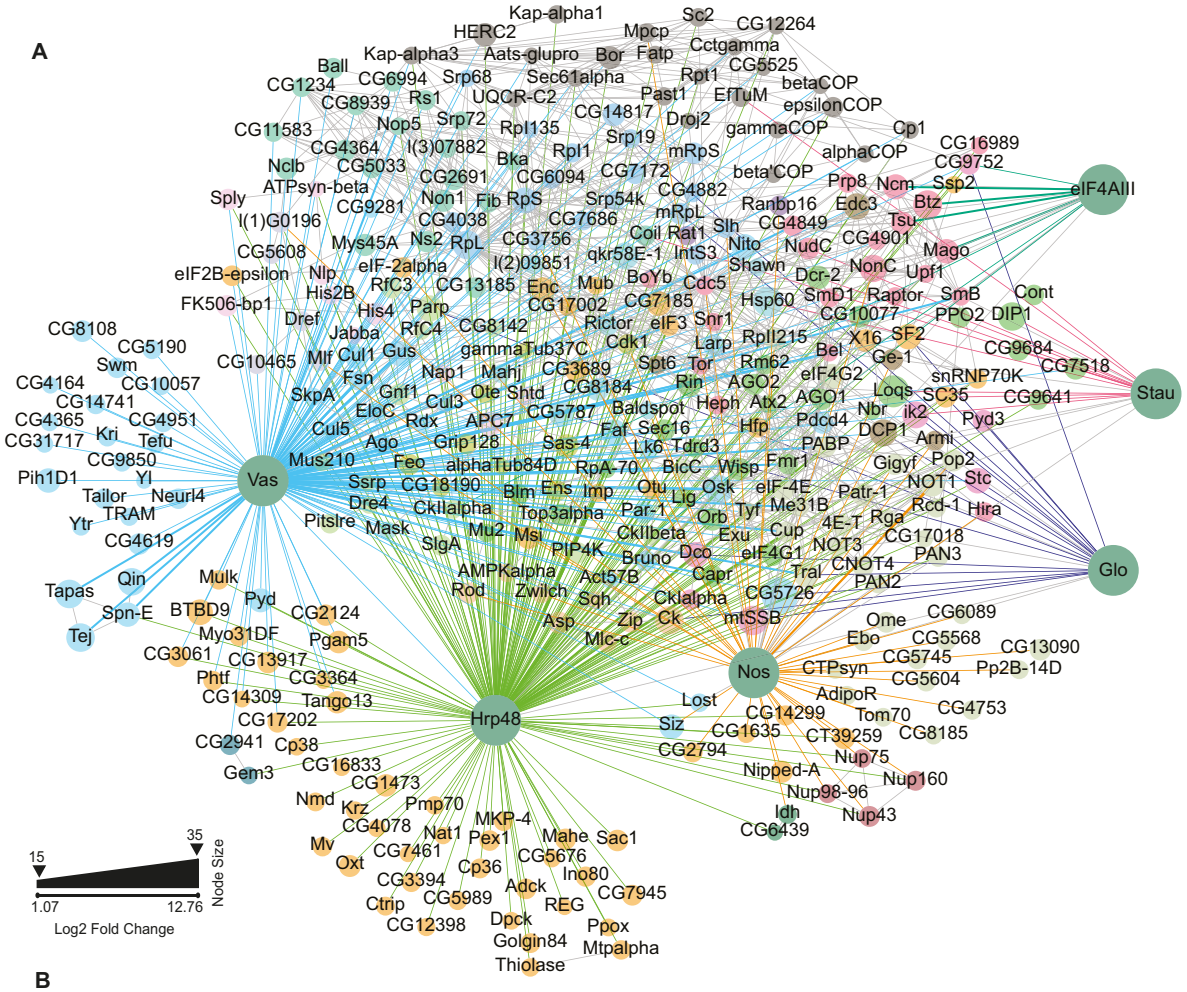
A
Vas
Hrp48
Nos
Stau
Glo
eIF4AIII
Node Size
15
35
1.07
12.76
Log2 Fold Change
B
GO Biological Process
GO:0002181 Cytoplasmic translation
GO:0051298 Centrosome duplication
GO:0032543 Mitochondrial translation
GO:0006413 Translational initiation
GO:0000027 Ribosomal large subunit assembly
GO:0001731 Formation of translation preinitiation complex
GO:0022008 Neurogenesis
GO:0000398 mRNA splicing, via spliceosome
GO:0017148 Negative regulation of translation
GO:0007095 Mitotic G2 DNA damage checkpoint
GO Cellular Compartment
GO:0005840 Ribosome
GO:0022625 Cytosolic large ribosomal subunit
GO:0000932 P-body
GO:0033290 Eukaryotic 48S preinitiation complex
GO:0005737 Cytoplasm
GO:0005852 Eukaryotic translation initiation factor 3 complex
GO:0005875 Microtubule associated complex
GO:0005730 Nucleolus
GO:0071013 Catalytic step 2 spliceosome
GO:0000228 Nuclear chromosome
GO Molecular Function
GO:0003735 Structural constituent of ribosome
GO:0003723 RNA binding
GO:0003729 mRNA binding
GO:0003743 Translation initiation factor activity
GO:0005515 Protein binding
GO:0019843 rRNA binding
GO:0005524 ATP binding
GO:0004535 poly(A)-specific ribonuclease activity
GO:0004004 ATP-dependent RNA helicase activity
GO:0070180 Large ribosomal subunit rRNA binding
0
20
40
60
-Log10 p-value

construct this network, we purified complexes associated with bait proteins, in an RNA-independent manner and used the MaxLFQ algorithm (84) for label-free relative protein quantification. The accuracy of this approach is comparable to labeled MS techniques such as SILAC (103). However, despite our stringent RNase treatment, it is possible that some of the recovered interactions are mediated by stretches of RNA protected from RNase cleavage by interacting proteins. By statistical filtering, we could separate background and specific binders for each bait. Several well characterized interactions were significantly enriched with most baits, indicating the efficacy of our workflow. To complement these data, we also obtained MS data from dimethyl labeling for a subset of the baits. We were able to validate 32 of the interactions assayed, including several novel associations.

In addition to the known regulators of mRNA localization and oocyte patterning, we co-purified nuclear and cytoplasmic complexes involved in different aspects of RNA metabolism. Our results highlight the diverse functions of these complexes in the post-transcriptional regulation of maternal mRNAs. The purification with the Stau-GFP bait of Loqs, a component of the RNA interference (RNAi) machinery is one such example. Loqs is a conserved cytoplasmic dsRBP. The protein participates in the biogenesis and processing of small noncoding RNAs that operate within the RNAi pathway (104). RNAi plays an important role in *Drosophila* germline development and the early phase of *osk* repression (96). *Drosophila Loqs* mutant females are sterile and their ovaries fail to sustain germ line stem cells (105). We found that both Dicer and Loqs are highly enriched in the Stau IP. We could confirm the Stau-Loqs interaction *in vitro*. This suggests a potential role for Stau in translational repression of *osk* by associating with the RNAi machinery. Although no such evidence has been presented in *Drosophila*, recent reports in other insects (*D. citri* and *L. decemlineata*) (106, 107) and the nematode *C. elegans* (11) have shown a requirement for Stau in RNAi responses. These results suggest a conserved role for Stau in RNAi-mediated gene silencing.

Nuclear Processing is Intrinsically Linked to Cytoplasmic Targeting of Maternal mRNAs—In addition to their crucial role in pre-mRNA processing, splicing factors also affect the cytoplasmic fates of mRNAs. SmB, a spliceosomal Sm protein is a known *osk* mRNP component. SmB contributes to germ-cell specification, at least in part by facilitating *osk* mRNA localization (95) and fails to localize to the posterior of the oocyte in the absence of Vas (108). Several Sm proteins have also been detected to be associated with Vas in the oocytes (56). Consistent with this, we co-purified SmB with Stau, Glo, Hrp48 and Vas. We also purified other splicing regulators with several of our baits, including Hfp (109) and the SR family proteins SC35 and SF2 (110, 111). Both SC35 and SF2 could be validated for their interaction with Glo and Stau, whereas Hfp bound eIF4AIII and Stau *in vitro*. Hfp was previously shown to interact with Hrp48 and Glo (38) and SF2 co-purifies with the short isoform of Osk (112). These results together with the well-studied role of SR proteins in cytoplasmic regulation of gene expression including mRNA export, decay, and translation in mammalian systems (113, 114) suggest that splicing factors are *bona fide* components of the mRNA localization machinery.

Translational Regulation of Maternal mRNAs by Hrp48 and Vas—In agreement with the function of Vas in enhancing the translation of maternal mRNAs (35, 36, 40, 49), we co-purified several ribosomal proteins and translation initiation factors with Vas-GFP. Our results suggest that Vas may recruit factors involved in translation initiation. This is also supported by the interaction of Vas with eIF5B and eIF3 subunits, as previously reported (56, 97–99).

In contrast to Vas, Hrp48 is a known translational repressor (45–47). In line with the localization of Hrp48 to P-bodies (115), we co-purified several components of the mRNA decay machinery, including the CCR4-NOT deadenylase complex with Hrp48-GFP. It is possible that these interactions are indirect and mediated by BicaudalC (BicC) and Belle (Bel). These proteins negatively regulate target mRNAs together with the CCR4-NOT complex (116, 117). We demonstrated *in vitro* binding of Hrp48 with both BicC and Bel. This suggests that by recruiting these proteins, Hrp48 may regulate the *nos* and *osk* mRNAs, possibly via CCR4-NOT mediated deadenylation (Fig. 8; ref. (116–119)). The function of Hrp48 in *nos* regulation remains to be investigated (Fig. 8).

However, the parallel enrichment of ribosomal proteins and P-body-components with Hrp48-GFP indicates its bifunctional role in modulating translation. Several lines of evidence from *Drosophila*, including binding of Hrp48 to a derepressor element in the *osk* 5'UTR (45), identification of Hrp48 as a part of a protein complex functioning in translational enhancement of *Hsp83* mRNA (120) and interaction of Hrp48

FIG. 4. **The global interactome reveals a connected network.** *A*, Interaction network of significantly enriched proteins, identified to be associated with each bait in the MS analysis. For Hrp48 and Vas, proteins from both labeled and label-free analyses were considered. Proteins are represented as nodes whereas edges represent the interactions. Green nodes represent the baits and the interactants are colored differently, based on their modularity class. The layout is based on a force-field analysis with the baits re-positioned for clarity. Edges representing interactions are colored differently for each bait: Vas in cyan; Hrp48 in green; eIF4AIII in dark green; Glo in blue; Stau in red; Nos in orange and databases in gray. The edges have a unit weight (representing a known interaction). Node size (except for baits) represents the fold change (Log2) over control. For simplicity, respective subunits of the eIF3 complex, cytoplasmic, and mitochondrial ribosomal proteins (separately for small and large subunits) were combined into a single node. *B*, Proteins were functionally annotated for their roles in biological processes, molecular functions and cellular components using GO term analysis. Only top ten terms in each category, with $p < 0.01$ are shown. The numbers represent the gene count involved in the respective GO term.

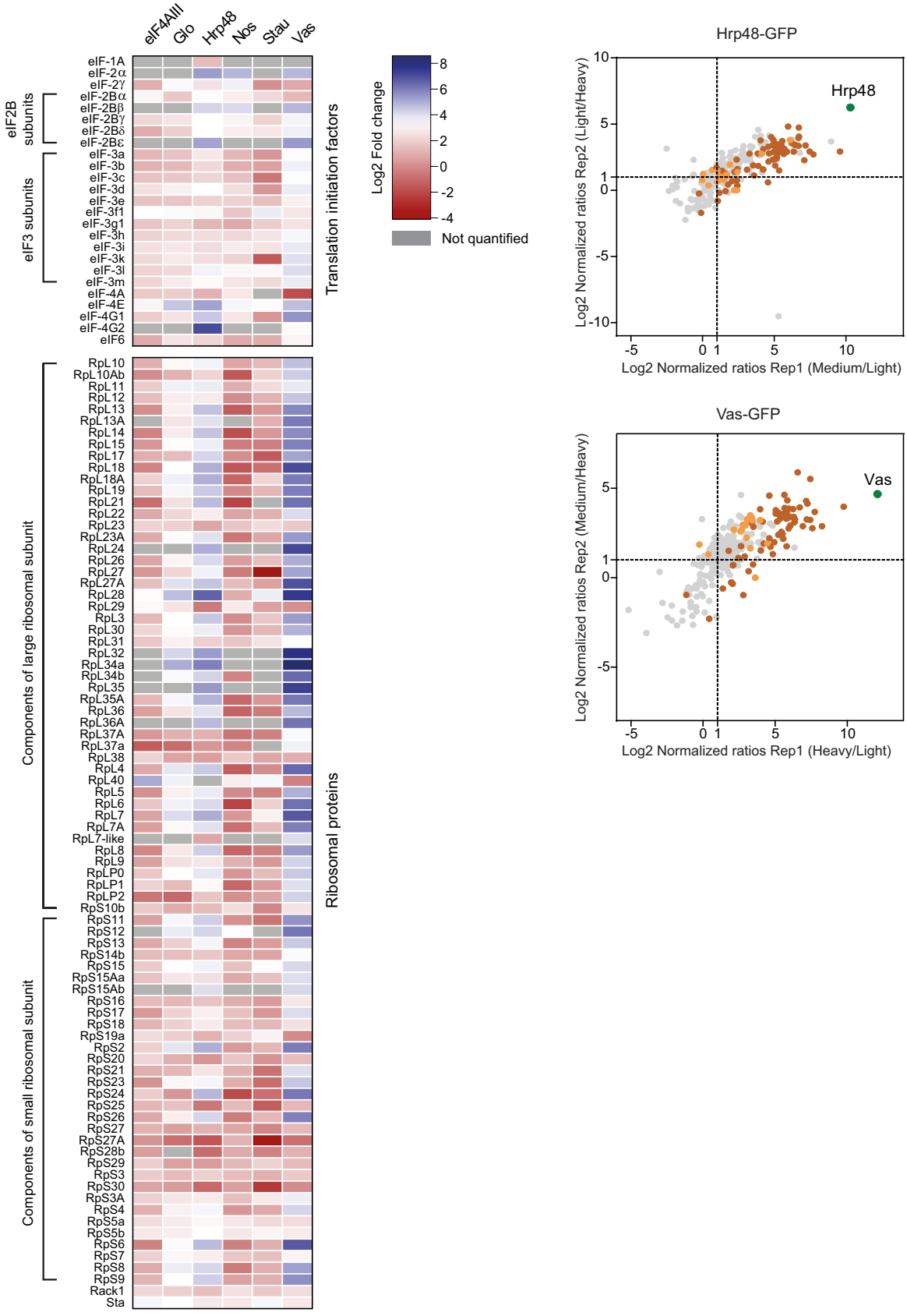
eIF4AIII
Glo
Hrp48
Nos
Stau
Vas
eIF2B subunits
eIF3 subunits
eIF-1A
eIF-2α
eIF-2γ
eIF-2Bα
eIF-2Bβ
eIF-2Bγ
eIF-2Bδ
eIF-2Bε
eIF-3a
eIF-3b
eIF-3c
eIF-3d
eIF-3e
eIF-3f1
eIF-3g1
eIF-3h
eIF-3i
eIF-3k
eIF-3l
eIF-3m
eIF-4A
eIF-4E
eIF-4G1
eIF-4G2
eIF6
Translation initiation factors
Log2 Fold change
8
6
4
2
0
-2
-4
Not quantified
Components of large ribosomal subunit
RpL10
RpL10Ab
RpL11
RpL12
RpL13
RpL13A
RpL14
RpL15
RpL17
RpL18
RpL18A
RpL19
RpL21
RpL22
RpL23
RpL23A
RpL24
RpL26
RpL27
RpL27A
RpL28
RpL29
RpL3
RpL30
RpL31
RpL32
RpL34a
RpL34b
RpL35
RpL35A
RpL36
RpL36A
RpL37A
RpL37a
RpL38
RpL4
RpL40
RpL5
RpL6
RpL7
RpL7A
RpL7-like
RpL8
RpL9
RpLP0
RpLP1
RpLP2
RpS10b
Components of small ribosomal subunit
RpS11
RpS12
RpS13
RpS14b
RpS15
RpS15Aa
RpS15Ab
RpS16
RpS17
RpS18
RpS19a
RpS2
RpS20
RpS21
RpS23
RpS24
RpS25
RpS26
RpS27
RpS27A
RpS28b
RpS29
RpS3
RpS30
RpS3A
RpS4
RpS5a
RpS5b
RpS6
RpS7
RpS8
RpS9
Rack1
Sta
Ribosomal proteins
Hrp48-GFP
Hrp48
Log2 Normalized ratios Rep2 (Light/Heavy)
Log2 Normalized ratios Rep1 (Medium/Light)
10
5
1
0
-5
-10
-5
0
1
5
10
Vas-GFP
Vas
Log2 Normalized ratios Rep2 (Medium/Heavy)
Log2 Normalized ratios Rep1 (Heavy/Light)

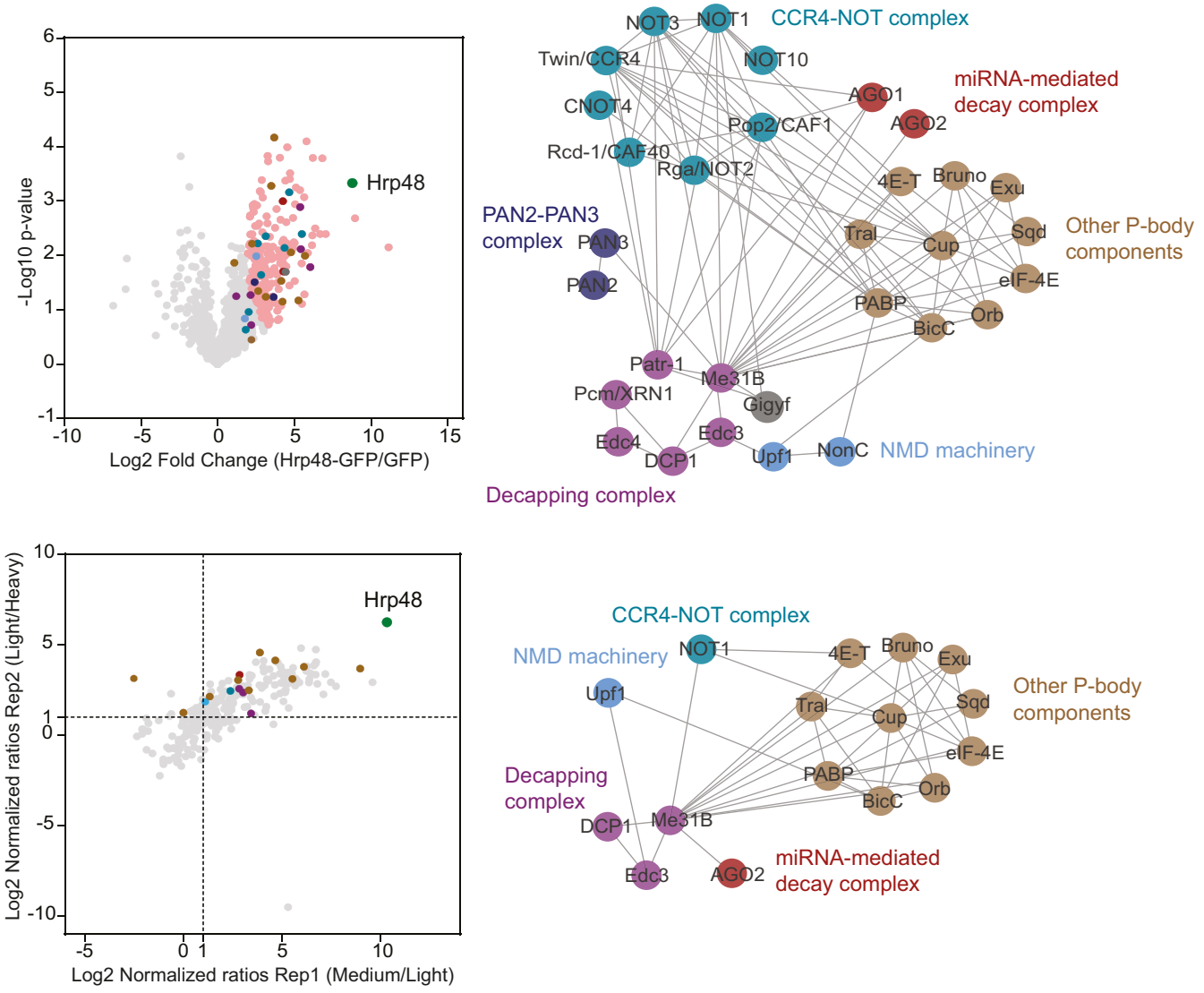

FIG. 6. **Several components of P-bodies, including the mRNA decay machinery were co-purified with Hrp48-GFP.** Volcano plot (*top*) and scatter plot (*bottom*) highlighting the distribution of different factors involved in translational repression/mRNA decay associated with Hrp48-GFP in the label-free and labeled MS analyses, respectively. Each identified protein is represented as a dot in light gray; the bait is highlighted in green; significantly enriched proteins are highlighted in pink; components of different complexes are highlighted in different colors as indicated in the subnetworks on the right. The subnetworks highlight the interactions between various components of distinct complexes, as previously reported in databases.

with CPEB (cytoplasmic polyadenylation element binding) protein Orb (this study) support the dual nature of Hrp48. hnRNP A2, the mammalian homolog of Hrp48, also exhibits the ability to mediate both translational stimulation (121) as well as repression (122), further strengthening the argument.

Identification of Novel Genes with a Potential Role in Drosophila Oogenesis—Along with several known regulators of maternal mRNAs, we identified the protein products of many previously uncharacterized genes. One such example is CG5726, which encodes for a protein with a MIF4G-like domain. This domain is found in many proteins involved in RNA metabolism including translation initiation factors, NMD factors and nuclear cap-binding proteins (65, 123–126). With no identifiable orthologs in humans, CG5726 protein shows up to 50%

FIG. 5. **Enrichment of ribosomal proteins and translation initiation factors for Vas-GFP and Hrp48-GFP.** On the left, heat map representation of the Log2 fold change of all ribosomal proteins and translation initiation factors co-purified with the six baits, in the label-free MS analysis. Gray rectangles represent empty values. On the right, scatter plots highlighting the distribution of ribosomal proteins and translation initiation factors found associated with Hrp48- and Vas-GFP in the dimethyl labeling analysis. Each identified protein is represented as a dot in light gray; baits are highlighted in green; ribosomal proteins are highlighted in brown; translation initiation factors are highlighted in orange.

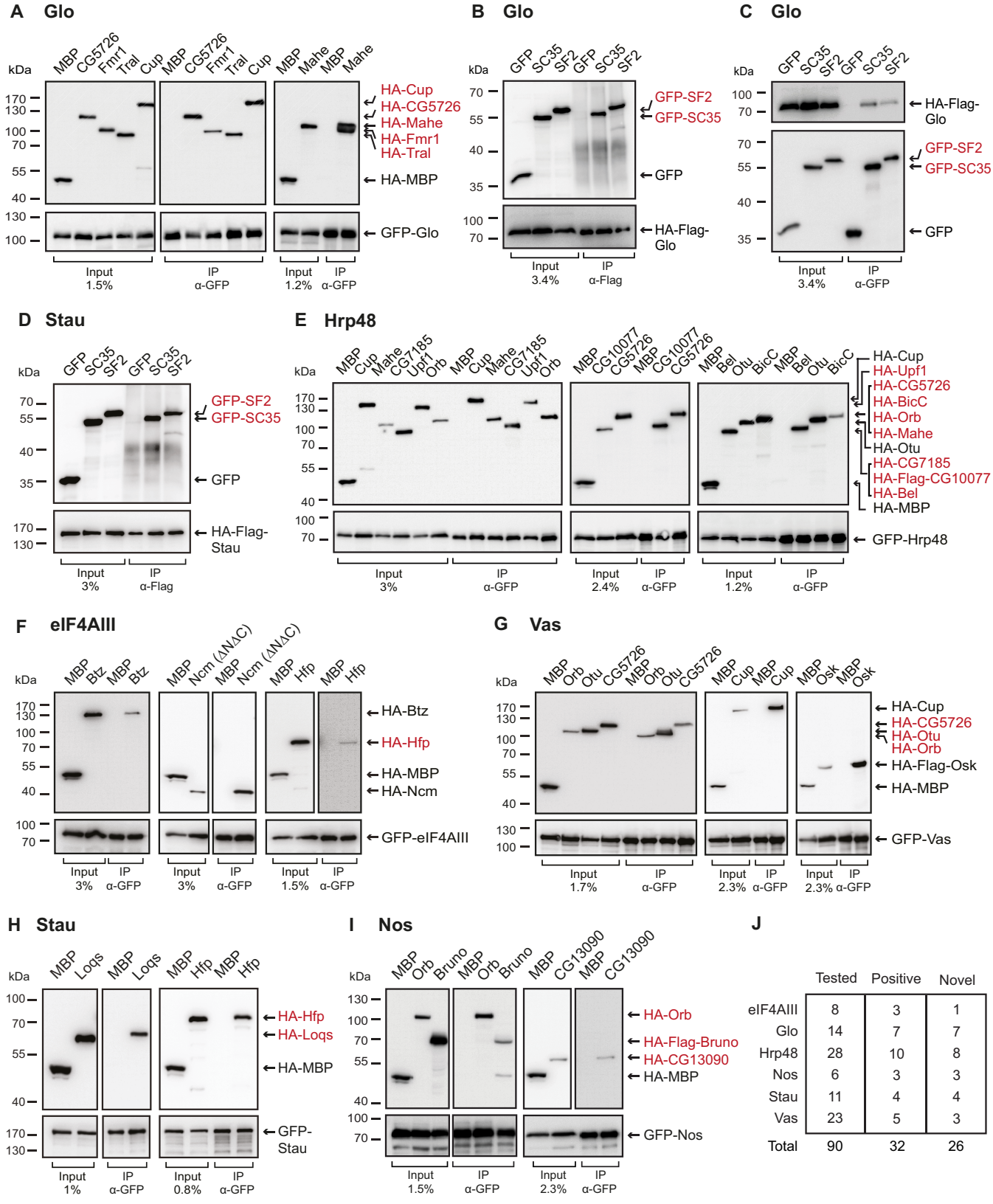

J

	Tested	Positive	Novel
eIF4AIII	8	3	1
Glo	14	7	7
Hrp48	28	10	8
Nos	6	3	3
Stau	11	4	4
Vas	23	5	3
Total	90	32	26

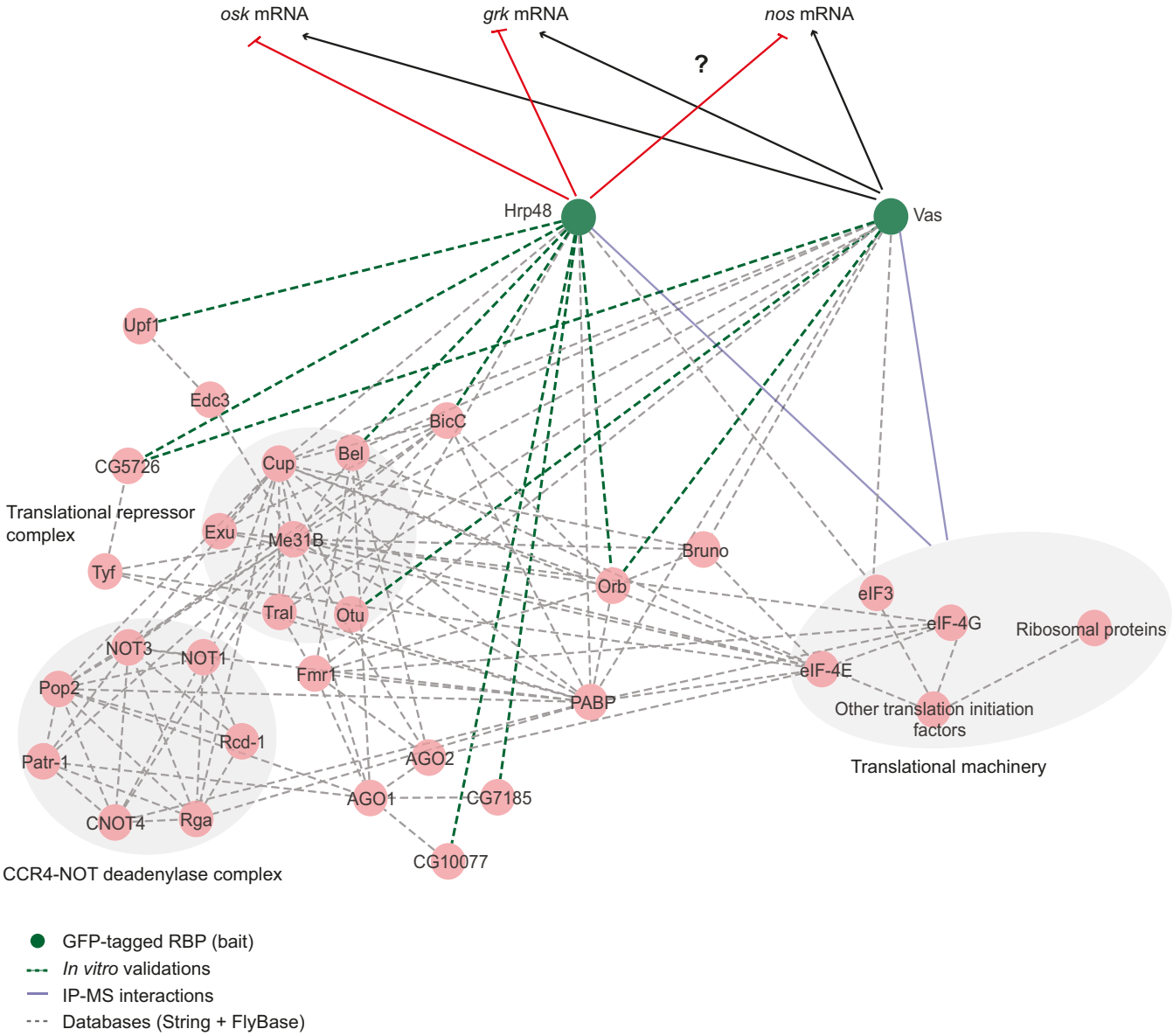

FIG. 8. **Model of Hrp48-mediated protein associations in the regulation of maternal mRNAs.** A subset of protein complexes interacting with Hrp48, possibly involved in the regulation of maternal mRNAs is shown. Many of these proteins were also found to be enriched in Vas-associated complexes. Note that only *in vitro* validated interactions of Hrp48 and Vas are shown here, except for their association with the translation machinery which was identified in the IP-MS data. Proteins are represented as circles and the interactions are represented as edges. Dotted gray lines represent the known interactions from databases; blue lines represent the interaction identified in the IP-MS data; green lines represent the *in vitro* validated novel interactions. Black arrows represent positive regulation whereas the red arrows represent negative regulation of mRNAs.

FIG. 7. ***In vitro* validation of interactions with bait proteins.** *A*, *E–I*, Lysates from human HEK293 cells expressing GFP-tagged baits and HA-tagged (or HA-Flag- tagged) candidates were immunoprecipitated using an anti-GFP nanobody coupled to magnetic beads. HA- tagged MBP served as a negative control. Inputs and eluates were analyzed by Western blotting using anti-GFP and anti-HA antibodies. For GFP-tagged proteins, 1–3% of the input and 10% of the eluates were loaded, whereas for HA-tagged (or HA-Flag- tagged) proteins, 1–3% of the input and 90% of the eluates were analyzed. *B*, *D*, HEK293 cells were co-transfected with HA-Flag-tagged baits and GFP-tagged candidates. GFP tag served as a control. Cell lysates were immunoprecipitated with anti-Flag antibody and analyzed by Western blotting. For HA-Flag-tagged proteins, 3–4% of the input and 10% of the eluates were loaded, whereas for GFP-tagged proteins, 3–4% of the input and 90% of the eluates were analyzed. *C*, Cells were transfected the same way as in panel B, and the lysate was immunoprecipitated with an anti-GFP nanobody coupled to magnetic beads. For GFP-tagged proteins, 3.4% of the input and 10% of the eluates were loaded, whereas for HA-Flag- tagged protein, 3.4% of the input and 90% of the eluates were analyzed. In each panel, cell lysates were treated with RNases before immunoprecipitation. Novel interactions are highlighted in red. *J*, Summary of interactions assayed by co-IPs in human HEK293 cells.

sequence identity among Drosophilids. In early embryos of *Drosophila melanogaster*, CG5726 interacts with short Osk (112). In this study, we found CG5726 to be interacting with multiple RBPs: Glo, Hrp48 and Vas, suggesting its possible role in translational regulation.

Consistent with the well-documented role of RNA helicases in oogenesis and fertility (88, 127–130), we identified two putative DEAD-box helicases, CG10077 and Mahe (Maheshvara). Although CG10077 is an ortholog of human DDX17, Mahe is an evolutionary conserved regulator of Notch signaling (131). We could recapitulate the interaction of Mahe with both Hrp48 and Glo, and CG10077 with Glo in our co-IP assay. Additionally, we found an interaction of CG13090 (Ubiquitin activating enzyme 4) with Nos. Mutations in this gene have been shown to impair ovarian stem cell functioning (132), which fits well with the role of Nos in maintenance of germline stem cells during oogenesis (53, 55). The functional characterization of the protein interactions uncovered in this work will require further *in vivo* studies.

With certain limitations such as partial functionality of bait proteins or loss of transient or weak interactions, our ability to recover many known associations and validation of several newly identified interactions indicates the general reliability of our data. Although we performed the experiments in a transcript-independent manner, cluster-based analysis of the complexes can be used to identify functional units potentially regulating different mRNAs. Integrating isolated complexes into interaction networks will further enable functional insights into poorly characterized proteins. Given the evolutionary conservation of several RBPs, our study provides a framework to transfer information to other systems, enhancing our understanding of regulation of RBPs and their diverse roles in developmental processes.

DATA AVAILABILITY

The MS proteomics data have been deposited to the ProteomeXchange Consortium via the PRIDE partner repository with the data set identifier PXD016680. The annotation spectra for the label-free MS have been deposited on MS-Viewer (http://msviewer.ucsf.edu/prospector/cgi-bin/msform.cgi?form=msviewer) and can be accessed by the search key "ydwohmubp3". The annotation data for dimethyl labeling MS are provided in supplemental Data S7.

Acknowledgments—We are grateful to Pavel Tomancak and Helena Jambor for their generous gifts of the fTRG fly stocks. We are particularly thankful to Gáspar Jékely for discussion and critical reading of the manuscript. We also thank Uwe Irion for discussions regarding the fly work; Elisa Izaurralde for mammalian cell expression vectors; Desiree Zerbst for providing clones for mammalian cell expression. This project received funding from Max Planck Gesellschaft, the European Research Council (ERC) under the European Union's Seventh Framework Program (FP7/2007-2013), ERC grant agreement no. 310957, and the Deutsche Forschungsgemeinschaft (FOR2333, BO3588/2-1 to F Bono).

Author contributions—P.B., B.M., and F.B. designed research; P.B., J.M., and K.S. performed research; P.B., B.M., and F.B. analyzed data; P.B., K.S., and F.B. wrote the paper; J.M. and K.S. contributed new reagents/analytic tools.

Conflict of interest—Authors declare no competing interests.

Abbreviations—The abbreviations used are: EGFP, enhanced green fluorescent protein; eIF, eukaryotic initiation factor; EJC, exon junction complex; FDR, false discovery rate; GO, gene ontology; HA, Hemagglutinin; hnRNP, heterogeneous nuclear ribonucleoproteins; IP, immunoprecipitation; LFQ, label-free quantification; MBP, maltose-binding protein; mRNP, messenger ribonucleoprotein; NMD, nonsense-mediated decay; PFA, paraformaldehyde; piRNA, piwi-interacting RNA; RBP, RNA-binding protein; SILAC, stable isotope labeling with amino acids; UAS, upstream activating sequence.

Received December 19, 2019, and in revised form, May 26, 2020
Published, MCP Papers in Press, June 17, 2020, DOI 10.1074/mcp.RA119.001912

REFERENCES

1. Moore, M. J., and Proudfoot, N. J. (2009) Pre-mRNA Processing Reaches Back toTranscription and Ahead to Translation. *Cell* **136,** 688–700
2. Singh, G., Pratt, G., Yeo, G. W., and Moore, M. J. (2015) The Clothes Make the mRNA: Past and Present Trends in mRNP Fashion. *Annu. Rev. Biochem*. **84,** 325–354
3. Hentze, M. W., Castello, A., Schwarzl, T., and Preiss, T. (2018) A brave new world of RNA-binding proteins. *Nat. Rev. Mol. Cell Biol*. **19,** 327–341
4. St Johnston, D., Beuchle, D., and Nüsslein-Volhard, C. (1991) staufen, a gene required to localize maternal RNAs in the Drosophila egg. *Cell* **66,** 51–63
5. Buchner, G., Bassi, M. T., Andolfi, G., Ballabio, A., and Franco, B. (1999) Identification of a novel homolog of the Drosophila staufen protein in the chromosome 8q13–q21.1 region. *Genomics* **62,** 113–118
6. Marión, R. M., Fortes, P., Beloso, A., Dotti, C., and Ortín, J. (1999) A human sequence homologue of Staufen is an RNA-binding protein that is associated with polysomes and localizes to the rough endoplasmic reticulum. *Mol. Cell Biol*. **19,** 2212–2219
7. Wickham, L., Duchaîne, T., Luo, M., Nabi, I. R., and DesGroseillers, L. (1999) Mammalian staufen is a double-stranded-RNA- and tubulin-binding protein which localizes to the rough endoplasmic reticulum. *Mol. Cell Biol*. **19,** 2220–2230
8. Yoon, Y. J., and Mowry, K. L. (2004) Xenopus Staufen is a component of a ribonucleoprotein complexcontaining Vg1 RNA and kinesin. *Development* **131,** 3035–3045
9. Bateman, M. J., Cornell, R., d'Alencon, C., and Sandra, A. (2004) Expression of the zebrafish Staufen gene in the embryo and adult. *Gene Expr. Patterns* **5,** 273–278
10. Liu, J., Hu, J. Y., Wu, F., Schwartz, J. H., and Schacher, S. (2006) Two mRNA-binding proteins regulate the distribution of syntaxin mRNA in Aplysia sensory neurons. *J. Neurosci*. **26,** 5204–5214
11. LeGendre, J. B., Campbell, Z. T., Kroll-Conner, P., Anderson, P., Kimble, J., and Wickens, M. (2013) RNA targets and specificity of Staufen, a double-stranded RNA-binding protein in Caenorhabditis elegans. *J. Biol. Chem*. **288,** 2532–2545

12. Schupbach, T., and Wieschaus, E. (1986) Maternal-effect mutations altering the anterior-posterior pattern of the Drosophila embryo. *Rouxs. Arch. Dev. Biol*. **195,** 302–317
13. Hay, B., Jan, L. Y., and Jan, Y. N. (1988) A protein component of Drosophila polar granules is encoded by vasa and has extensive sequence similarity to ATP-dependent helicases. *Cell* **55,** 577–587
14. Lasko, P. F., and Ashburner, M. (1988) The product of the Drosophila gene vasa is very similar to eukaryotic initiation factor-4A. *Nature* **335,** 611–617
15. Komiya, T., Itoh, K., Ikenishi, K., and Furusawa, M. (1994) Isolation and characterization of a novel gene of the DEAD box protein family which is specifically expressed in germ cells of Xenopus laevis. *Dev. Biol*. **162,** 354–363
16. Fujiwara, Y., Komiya, T., Kawabata, H., Sato, M., Fujimoto, H., Furusawa, M., and Noce, T. (1994) Isolation of a DEAD-family protein gene that encodes a murine homolog of Drosophila vasa and its specific expression in germ cell lineage. *Proc. Natl. Acad. Sci. U.S.A*. **91,** 12258–12262
17. Komiya, T., and Tanigawa, Y. (1995) Cloning of a gene of the dead box protein family which is specifically expressed in germ cells in rats. *Biochem. Biophys. Res. Commun*. **207,** 405–410
18. Gruidl, M. E., Smith, P. A., Kuznicki, K. A., McCrone, J. S., Kirchner, J., Roussell, D. L., Strome, S., and Bennett, K. L. (1996) Multiple potential germ-line helicases are components of the germ-line-specific P granules of Caenorhabditis elegans. *Proc. Natl. Acad. Sci. U.S.A*. **93,** 13837–13842
19. Yoon, C., Kawakami, K., Hopkins, N., Alberts, B. M., and Jan, Y. N. (1997) Zebrafish vasa homologue RNA is localized to the cleavage planes of 2- and 4-cell-stage embryos and is expressed in the primordial germ cells. *Development* **124,** 3157–3165
20. Tsunekawa, N., Naito, M., Sakai, Y., Nishida, T., and Noce, T. (2000) Isolation of chicken vasa homolog gene and tracing the origin of primordial germ cells. *Development* **127,** 2741–2750
21. Owttrim, G. W., Mandel, T., Trachsel, H., Thomas, A. A. M., and Kuhlemeier, C. (1994) Characterization of the tobacco eIF-4A gene family. *Plant Mol. Biol*. **26,** 1747–1757
22. Weinstein, D. C., Honore, E., and Hemmati-Brivanlou, A. (1997) Epidermal induction and inhibition of neural fate by translation initiation factor 4AIII. *Development* **124,** 4235–4242
23. Kressler, D., de la Cruz, J., Rojo, M., and Linder, P. (1997) Fal1p is an essential DEAD-box protein involved in 40S-ribosomal-subunit biogenesis in Saccharomyces cerevisiae. *Mol. Cell Biol*. **17,** 7283–7294
24. Li, Q., Imataka, H., Morino, S., Rogers, G. W., Richter-Cook, N. J., Merrick, W. C., and Sonenberg, N. (1999) Eukaryotic translation initiation factor 4AIII (eIF4AIII) is functionally distinct from eIF4AI and eIF4AII. *Mol. Cell Biol*. **19,** 7336–7346
25. Palacios, I. M., Gatfield, D., St Johnston, D., and Izaurralde, E. (2004) An eIF4AIII-containing complex required for mRNA localization and nonsense-mediated mRNA decay. *Nature* **427,** 753–757
26. Lehmann, R., and Nusslein-Volhard, C. (1991) The maternal gene nanos has a central role in posterior pattern formation of the Drosophila embryo. *Development* **112,** 679–691
27. Subramaniam, K., and Seydoux, G. (1999) nos-1 and nos-2, two genes related to Drosophila nanos, regulate primordial germ cell development and survival in Caenorhabditis elegans. *Development* **126,** 4861–4871
28. MacArthur, H., Bubunenko, M., Houston, D. W., and King, M. L. (1999) Xcat2 RNA is a translationally sequestered germ plasm component in Xenopus. *Mech. Dev*. **84,** 75–88
29. Köprunner, M., Thisse, C., Thisse, B., and Raz, E. (2001) A zebrafish nanos-related gene is essential for the development of primordial germ cells. *Genes Dev*. **15,** 2877–2885
30. Tsuda, M., Sasaoka, Y., Kiso, M., Abe, K., Haraguchi, S., Kobayashi, S., and Saga, Y. (2003) Conserved role of nanos proteins in germ cell development. *Science*. **301,** 1239–1241
31. Matunis, M. J., Matunis, E. L., and Dreyfuss, G. (1992) Isolation of hnRNP complexes from Drosophila melanogaster. *J. Cell Biol*. **116,** 245–255
32. Matunis, E. L., Matunis, M. J., and Dreyfuss, G. (1992) Characterization of the major hnRNP proteins from Drosophila melanogaster. *J. Cell Biol*. **116,** 257–269
33. Piccolo, L. L., Corona, D., and Onorati, M. C. (2014) Emerging Roles for hnRNPs in post-transcriptional regulation: what can we learn from flies? *Chromosoma* **123,** 515–527
34. Kim-Ha, J., Smith, J. L., and Macdonald, P. M. (1991) oskar mRNA is localized to the posterior pole of the Drosophila oocyte. *Cell* **66,** 23–35
35. Styhler, S., Nakamura, A., Swan, A., Suter, B., and Lasko, P. (1998) vasa is required for GURKEN accumulation in the oocyte, and is involved in oocyte differentiation and germline cyst development. *Development* **125,** 1569–1578
36. Tomancak, P., Guichet, A., Zavorszky, P., and Ephrussi, A. (1998) Oocyte polarity depends on regulation of gurken by Vasa. *Development* **125,** 1723–1732
37. Huynh, J.-R., Munro, T. P., Smith-Litière, K., Lepesant, J.-A., and Johnston, D. S. (2004) The Drosophila hnRNPA/B homolog, Hrp48, is specifically required for a distinct step in osk mRNA localization. *Dev. Cell*. **6,** 625–635
38. Kalifa, Y., Armenti, S. T., and Gavis, E. R. (2009) Glorund interactions in the regulation of gurken and oskar mRNAs. *Dev. Biol*. **326,** 68–74
39. Ephrussi, A., and Lehmann, R. (1992) Induction of germ cell formation by oskar. *Nature* **358,** 387–392
40. Markussen, F. H., Michon, A. M., Breitwieser, W., and Ephrussi, A. (1995) Translational control of oskar generates short OSK, the isoform that induces pole plasma assembly. *Development* **121,** 3723–3732
41. Breitwieser, W., Markussen, F. H., Horstmann, H., and Ephrussi, A. (1996) Oskar protein interaction with Vasa represents an essential step in polar granule assembly. *Genes Dev*. **10,** 2179–2188
42. Rongo, C., Broihier, H. T., Moore, L., Van Doren, M., Forbes, A., and Lehmann, R. (1997) Germ plasm assembly and germ cell migration in Drosophila. *Cold Spring Harb. Symp. Quant. Biol*. **62,** 1–11
43. St Johnston, D., Driever, W., Berleth, T., Richstein, S., and Nüsslein-Volhard, C. (1989) Multiple steps in the localization of bicoid RNA to the anterior pole of the Drosophila oocyte. *Development* **107,** 13–19
44. Ferrandon, D., Elphick, L., Nüsslein-Volhard, C., and St Johnston, D. (1994) Staufen protein associates with the 3′UTR of bicoid mRNA to form particles that move in a microtubule-dependent manner. *Cell* **79,** 1221–1232
45. Gunkel, N., Yano, T., Markussen, F.-H., Olsen, L. C., and Ephrussi, A. (1998) Localization-dependent translation requires a functional interaction between the 5' and 3' ends of oskar mRNA. *Genes Dev*. **12,** 1652–1664
46. Yano, T., de Quinto, S. L., Matsui, Y., Shevchenko, A., Shevchenko, A., and Ephrussi, A. (2004) Hrp48, a Drosophila hnRNPA/B homolog, binds and regulates translation of oskar mRNA. *Dev. Cell*. **6,** 637–648
47. Goodrich, J. S., Clouse, K. N., and Schüpbach, T. (2004) Hrb27C, Sqd and Otu cooperatively regulate gurken RNA localization and mediate nurse cell chromosome dispersion in Drosophila oogenesis. *Development* **131,** 1949–1958
48. Kalifa, Y., Huang, T., Rosen, L. N., Chatterjee, S., and Gavis, E. R. (2006) Glorund, a Drosophila hnRNP F/H homolog, is an ovarian repressor of nanos translation. *Dev. Cell*. **10,** 291–301
49. Gavis, E. R., Lunsford, L., Bergsten, S. E., and Lehmann, R. (1996) A conserved 90 nucleotide element mediates translational repression of nanos RNA. *Development* **122,** 2791–2800
50. Siebel, C. W., Kanaar, R., and Rio, D. C. (1994) Regulation of tissue-specific P-element pre-mRNA splicing requires the RNA-binding protein PSI. *Genes Dev*. **8,** 1713–1725
51. Hammond, L. E., Rudner, D. Z., Kanaar, R., and Rio, D. C. (1997) Mutations in the hrp48 gene, which encodes a Drosophila heterogeneous nuclear ribonucleoprotein particle protein, cause lethality and developmental defects and affect P-element third-intron splicing in vivo. *Mol. Cell Biol*. **17,** 7260–7267
52. Burnette, J. M., Hatton, A. R., and Lopez, A. J. (1999) Trans-acting factors required for inclusion of regulated exons in the Ultrabithorax mRNAs of Drosophila melanogaster. *Genetics* **151,** 1517–1529
53. Forbes, A., and Lehmann, R. (1998) Nanos and Pumilio have critical roles in the development and function of Drosophila germline stem cells. *Development* **125,** 679–690
54. Bhat, K. M. (1999) The posterior determinant gene nanos is required for the maintenance of the adult germline stem cells during Drosophila oogenesis. *Genetics* **151,** 1479–1492
55. Wang, Z., and Lin, H. (2004) Nanos maintains germline stem cell self-renewal by preventing differentiation. *Science* **303,** 2016–2019
56. Durdevic, Z., and Ephrussi, A. (2019) Germ cell lineage homeostasis in Drosophila requires the Vasa RNA helicase. *Genetics, genetics* **213,** 911–922

57. Kobayashi, S., Yamada, M., Asaoka, M., and Kitamura, T. (1996) Essential role of the posterior morphogen nanos for germline development in Drosophila. *Nature* **380,** 708–711
58. Asaoka, M., Sano, H., Obara, Y., and Kobayashi, S. (1998) Maternal Nanos regulates zygotic gene expression in germline progenitors of Drosophila melanogaster. *Mech. Dev*. **78,** 153–158
59. Deshpande, G., Calhoun, G., Yanowitz, J. L., and Schedl, P. D. (1999) Novel functions of nanos in downregulating mitosis and transcription during the development of the Drosophila germline. *Cell* **99,** 271–281
60. Hayashi, Y., Hayashi, M., and Kobayashi, S. (2004) Nanos suppresses somatic cell fate in Drosophila germ line. *Proc. Natl. Acad. Sci. U.S.A*. **101,** 10338–10342
61. Sato, K., Hayashi, Y., Ninomiya, Y., Shigenobu, S., Arita, K., Mukai, M., and Kobayashi, S. (2007) Maternal Nanos represses hid/skl-dependent apoptosis to maintain the germ line in Drosophila embryos. *Proc. Natl. Acad. Sci. U.S.A*. **104,** 7455–7460
62. Wang, C., Dickinson, L. K., and Lehmann, R. (1994) Genetics of nanos Localization in Drosophila. *Dev. Dyn*. **199,** 103–115
63. Heraud-Farlow, J. E., and Kiebler, M. A. (2014) The multifunctional Staufen proteins: conserved roles from neurogenesis to synaptic plasticity. *Trends Neurosci*. **37,** 470–479
64. De Keuckelaere, E., Hulpiau, P., Saeys, Y., Berx, G., and van Roy, F. (2018) Nanos genes and their role in development and beyond. *Cell. Mol. Life Sci*. **75,** 1929–1946
65. Buchwald, G., Schüssler, S., Basquin, C., Le Hir, H., and Conti, E. (2013) Crystal structure of the human eIF4AIII–CWC22 complex shows how a DEAD-box protein is inhibited by a MIF4G domain. *Proc. Natl. Acad. Sci. U.S.A*. **110,** E4611–E4618
66. Sarov, M., Barz, C., Jambor, H., Hein, M. Y., Schmied, C., Suchold, D., Stender, B., Janosch, S., K J, V. V., Krishnan, R. T., Krishnamoorthy, A., Ferreira, I. R. S., Ejsmont, R. K., Finkl, K., Hasse, S., Kämpfer, P., Plewka, N., Vinis, E., Schloissnig, S., Knust, E., Hartenstein, V., Mann, M., Ramaswami, M., VijayRaghavan, K., Tomancak, P., and Schnorrer, F. (2016) A genome-wide resource for the analysis of protein localisation in Drosophila. *Elife*. **5,** e12068
67. Lazzaretti, D., Veith, K., Kramer, K., Basquin, C., Urlaub, H., Irion, U., and Bono, F. (2016) The bicoid mRNA localization factor Exuperantia is an RNA-binding pseudonuclease. *Nat. Struct. Mol. Biol*. **23,** 705–713
68. Rappsilber, J., Mann, M., and Ishihama, Y. (2007) Protocol for micro-purification, enrichment, pre-fractionation and storage of peptides for proteomics using StageTips. *Nat. Protoc*. **2,** 1896–1906
69. Semanjski, M., Germain, E., Bratl, K., Kiessling, A., Gerdes, K., and Macek, B. (2018) The kinases HipA and HipA7 phosphorylate different substrate pools in *Escherichia coli* to promote multidrug tolerance. *Sci. Signal*. **11,** eaat5750
70. Boersema, P. J., Raijmakers, R., Lemeer, S., Mohammed, S., and Heck, A. J. R. (2009) Multiplex peptide stable isotope dimethyl labeling for quantitative proteomics. *Nat. Protoc*. **4,** 484–494
71. Cox, J., Neuhauser, N., Michalski, A., Scheltema, R. A., Olsen, J. V., and Mann, M. (2011) Andromeda: a peptide search engine integrated into the MaxQuant Environment. *J. Proteome Res*. **10,** 1794–1805
72. Elias, J. E., and Gygi, S. P. (2010) Target-decoy search strategy for mass spectrometry-based proteomics. *Methods Mol. Biol*. **604,** 55–71
73. Tyanova, S., Temu, T., and Cox, J. (2016) The MaxQuant computational platform for mass spectrometry-based shotgun proteomics. *Nat. Protoc*. **11,** 2301–2319
74. Cox, J., and Mann, M. (2008) MaxQuant enables high peptide identification rates, individualized p.p.b.-range mass accuracies and proteome-wide protein quantification. *Nat. Biotechnol*. **26,** 1367–1372
75. Shannon, P., Markiel, A., Ozier, O., Baliga, N. S., Wang, J. T., Ramage, D., Amin, N., Schwikowski, B., and Ideker, T. (2003) Cytoscape: a software environment for integrated models of biomolecular interaction networks. *Genome Res*. **13,** 2498–2504
76. Szklarczyk, D., Gable, A. L., Lyon, D., Junge, A., Wyder, S., Huerta-Cepas, J., Simonovic, M., Doncheva, N. T., Morris, J. H., Bork, P., Jensen, L. J., and Mering, C. V. (2019) STRING v11: protein–protein association networks with increased coverage, supporting functional discovery in genome-wide experimental datasets. *Nucleic Acids Res*. **47,** D607–D613
77. Thurmond, J., Goodman, J. L., Strelets, V. B., Attrill, H., Gramates, L. S., Marygold, S. J., Matthews, B. B., Millburn, G., Antonazzo, G., Trovisco, V., Kaufman, T. C., Calvi, B. R., Perrimon, N., Gelbart, S. R., Agapite, J., Broll, K., Crosby, L., Santos, G. D., Emmert, D., Gramates, L. S., Falls, K., Jenkins, V., Matthews, B., Sutherland, C., Tabone, C., Zhou, P., Zytkovicz, M., Brown, N., Antonazzo, G., Attrill, H., Garapati, P., Holmes, A., Larkin, A., Marygold, S., Millburn, G., Pilgrim, C., Trovisco, V., Urbano, P., Kaufman, T., Calvi, B., Czoch, B., Goodman, J., Strelets, V., Thurmond, J., Cripps, R., and Baker, P, FlyBase Consortium, (2019) FlyBase 2.0: the next generation. *Nucleic Acids Res*. **47,** D759–D765
78. Bastian, M., Heymann, S., and Jacomy, M. (2009) Gephi : an open source software for exploring and manipulating networks. *International AAAI Conference on Weblogs and Social Media*
79. Blondel, V. D., Guillaume, J.-L., Lambiotte, R., and Lefebvre, E. (2008) Fast unfolding of communities in large networks. *J. Stat. Mech. Theory*. **2008,** P10008
80. Huang, D. W., Sherman, B. T., and Lempicki, R. A. (2009) Systematic and integrative analysis of large gene lists using DAVID bioinformatics resources. *Nat. Protoc*. **4,** 44–57
81. Huang, D. W., Sherman, B. T., and Lempicki, R. A. (2009) Bioinformatics enrichment tools: paths toward the comprehensive functional analysis of large gene lists. *Nucleic Acids Res*. **37,** 1–13
82. Supek, F., Bošnjak, M., Škunca, N., and Šmuc, T. (2011) REVIGO summarizes and visualizes long lists of gene ontology terms. *PLoS ONE*. **6,** e21800
83. Liang, L., Diehl-Jones, W., and Lasko, P. (1994) Localization of vasa protein to the Drosophila pole plasm is independent of its RNA-binding and helicase activities. *Development* **120,** 1201–1211
84. Cox, J., Hein, M. Y., Luber, C. A., Paron, I., Nagaraj, N., and Mann, M. (2014) Accurate proteome-wide label-free quantification by delayed normalization and maximal peptide ratio extraction, Termed MaxLFQ. *Mol. Cell. Proteomics* **13,** 2513–2526
85. Velentzas, A. D., Anagnostopoulos, A. K., Velentzas, P. D., Mpakou, V. E., Sagioglou, N. E., Tsioka, M. M., Katarachia, S., Manta, A. K., Konstantakou, E. G., Papassideri, I. S., Tsangaris, G. T. H., and Stravopodis, D. J. (2015) Global proteomic profiling of Drosophila ovary: a high-resolution, unbiased, accurate and multifaceted analysis. *Cancer Genomics Proteomics*. **12,** 369–384
86. Kadyrova, L. Y., Habara, Y., Lee, T. H., and Wharton, R. P. (2007) Translational control of maternal Cyclin B mRNA by Nanos in the Drosophila germline. *Development* **134,** 1519–1527
87. Raisch, T., Bhandari, D., Sabath, K., Helms, S., Valkov, E., Weichenrieder, O., and Izaurralde, E. (2016) Distinct modes of recruitment of the CCR4-NOT complex by Drosophila and vertebrate Nanos. *EMBO J*. **35,** 974–990
88. Dehghani, M., and Lasko, P. (2017) Multiple functions of the DEAD-box helicase Vasa in *Drosophila* oogenesis. In: Kloc M. (eds) *Oocytes. Results and Problems in Cell Differentiation*, vol **63**. Springer, Cham
89. Clouse, K. N., Ferguson, S. B., and Schüpbach, T. (2008) Squid, Cup, and PABP55B function together to regulate gurken translation in Drosophila. *Dev. Biol*. **313,** 713–724
90. McDermott, S. M., Meignin, C., Rappsilber, J., and Davis, I. (2012) Drosophila Syncrip binds the gurken mRNA localisation signal and regulates localised transcripts during axis specification. *Biol. Open*. **1,** 488–497
91. Kugler, J.-M., Woo, J.-S., Oh, B.-H., and Lasko, P. (2010) Regulation of Drosophila Vasa in vivo through paralogous Cullin-RING E3 ligase specificity receptors. *Mol. Cell Biol*. **30,** 1769–1782
92. Nishida, K. M., Okada, T. N., Kawamura, T., Mituyama, T., Kawamura, Y., Inagaki, S., Huang, H., Chen, D., Kodama, T., Siomi, H., and Siomi, M. C. (2009) Functional involvement of Tudor and dPRMT5 in the piRNA processing pathway in Drosophila germlines. *EMBO J*. **28,** 3820–3831
93. Webster, A., Li, S., Hur, J. K., Wachsmuth, M., Bois, J. S., Perkins, E. M., Patel, D. J., and Aravin, A. A. (2015) Aub and Ago3 Are recruited to Nuage through two mechanisms to form a ping-pong complex assembled by Krimper. *Mol. Cell*. **59,** 564–575
94. Guruharsha, K. G., Rual, J.-F., Zhai, B., Mintseris, J., Vaidya, P., Vaidya, N., Beekman, C., Wong, C., Rhee, D. Y., Cenaj, O., McKillip, E., Shah, S., Stapleton, M., Wan, K. H., Yu, C., Parsa, B., Carlson, J. W., Chen, X., Kapadia, B., VijayRaghavan, K., Gygi, S. P., Celniker, S. E., Obar, R. A., and Artavanis-Tsakonas, S. (2011) A protein complex network of Drosophila melanogaster. *Cell* **147,** 690–703
95. Gonsalvez, G. B., Rajendra, T. K., Wen, Y., Praveen, K., and Matera, A. G. (2010) Sm proteins specify germ cell fate by facilitating oskar mRNA localization. *Development* **137,** 2341–2351

96. Kugler, J. M., and Lasko, P. (2009) Localization, anchoring and translational control of oskar, gurken, bicoid and nanos mRNA during drosophila oogenesis. *Fly. (Austin)*. **3,** 15–28
97. Carrera, P., Johnstone, O., Nakamura, A., Casanova, J., Jäckle, H., and Lasko, P. (2000) VASA mediates translation through interaction with a Drosophila yIF2 homolog. *Mol. Cell*. **5,** 181–187
98. Johnstone, O., and Lasko, P. (2004) Interaction with eIF5B is essential for Vasa function during development. *Development* **131,** 4167–4178
99. Liu, N., Han, H., and Lasko, P. (2009) Vasa promotes Drosophila germline stem cell differentiation by activating mei-P26 translation by directly interacting with a (U)-rich motif in its 3' UTR. *Genes Dev*. **23,** 2742–2752
100. Thomson, T., Liu, N., Arkov, A., Lehmann, R., and Lasko, P. (2008) Isolation of new polar granule components in Drosophila reveals P body and ER associated proteins. *Mech. Dev*. **125,** 865–873
101. Szostak, E., García-Beyaert, M., Guitart, T., Graindorge, A., Coll, O., and Gebauer, F. (2018) Hrp48 and eIF3d contribute to msl-2 mRNA translational repression. *Nucleic Acids Res*. **46,** 4099–4113
102. Franco, M., Seyfried, N. T., Brand, A. H., Peng, J., and Mayor, U. (2011) A novel strategy to isolate ubiquitin conjugates reveals wide role for ubiquitination during neural development. *Mol. Cell. Proteomics* **10,** M110.002188
103. Eberl, H. C., Spruijt, C. G., Kelstrup, C. D., Vermeulen, M., and Mann, M. (2013) A map of general and specialized chromatin readers in mouse tissues generated by label-free interaction proteomics. *Mol. Cell*. **49,** 368–378
104. Fukunaga, R., and Zamore, P. D. (2012) Loquacious, a dicer partner protein, functions in both the MicroRNA and siRNA. *Pathways. Enzym*. **32,** 37–68
105. Förstemann, K., Tomari, Y., Du, T., Vagin, V. V., Denli, A. M., Bratu, D. P., Klattenhoff, C., Theurkauf, W. E., and Zamore, P. D. (2005) Normal microRNA maturation and germ-line stem cell maintenance requires loquacious, a double-stranded RNA-binding domain protein. *PLos Biol*. **3,** e236
106. Taning, C. N. T., Andrade, E. C., Hunter, W. B., Christiaens, O., and Smagghe, G. (2016) Asian Citrus Psyllid RNAi Pathway – RNAi evidence. *Sci. Rep*. **6,** 38082
107. Yoon, J.-S., Mogilicherla, K., Gurusamy, D., Chen, X., Chereddy, S. C. R. R., and Palli, S. R. (2018) Double-stranded RNA binding protein, Staufen, is required for the initiation of RNAi in coleopteran insects. *Proc. Natl. Acad. Sci. U.S.A*. **115,** 8334–8339
108. Anne, J. (2010) Arginine methylation of SmB is required for Drosophila germ cell development. *Development* **137,** 2819–2828
109. Van Buskirk, C., and Schüpbach, T. (2002) Half pint regulates alternative splice site selection in Drosophila. *Dev. Cell*. **2,** 343–353
110. Krainer, A. R., Conway, G. C., and Kozak, D. (1990) The essential pre-mRNA splicing factor SF2 influences 5' splice site selection by activating proximal sites. *Cell* **62,** 35–42
111. Ge, H., and Manley, J. L. (1990) A protein factor, ASF, controls cell-specific alternative splicing of SV40 early pre-mRNA in vitro. *Cell* **62,** 25–34
112. Hurd, T. R., Herrmann, B., Sauerwald, J., Sanny, J., Grosch, M., and Lehmann, R. (2016) Long Oskar controls mitochondrial inheritance in Drosophila melanogaster. *Dev. Cell*. **39,** 560–571
113. Long, J. C., and Caceres, J. F. (2009) The SR protein family of splicing factors: Master regulators of gene expression. *Biochem. J*. **417,** 15–27
114. Jeong, S. (2017) SR proteins: Binders, regulators, and connectors of RNA. *Mol. Cells*. **40,** 1–9
115. Weil, T. T., Parton, R. M., Herpers, B., Soetaert, J., Veenendaal, T., Xanthakis, D., Dobbie, I. M., Halstead, J. M., Hayashi, R., Rabouille, C., and Davis, I. (2012) Drosophila patterning is established by differential association of mRNAs with P bodies. *Nat. Cell Biol*. **14,** 1305–1313
116. Chicoine, J., Benoit, P., Gamberi, C., Paliouras, M., Simonelig, M., and Lasko, P. (2007) Bicaudal-C recruits CCR4-NOT deadenylase to target mRNAs and regulates oogenesis, cytoskeletal organization, and its own expression. *Dev. Cell*. **13,** 691–704
117. Götze, M., Dufourt, J., Ihling, C., Rammelt, C., Pierson, S., Sambrani, N., Temme, C., Sinz, A., Simonelig, M., and Wahle, E. (2017) Translational repression of the *Drosophila nanos* mRNA involves the RNA helicase Belle and RNA coating by Me31B and Trailer hitch. *RNA* **23,** 1552–1568
118. Mahone, M., Saffman, E. E., and Lasko, P. F. (1995) Localized Bicaudal-C RNA encodes a protein containing a KH domain, the RNA binding motif of FMR1. *EMBO J*. **14,** 2043–2055
119. Saffman, E. E., Styhler, S., Rother, K., Li, W., Richard, S., and Lasko, P. (1998) Premature translation of oskar in oocytes lacking the RNA-binding protein bicaudal-C. *Mol. Cell Biol*. **18,** 4855–4862
120. Nelson, M. R., Luo, H., Vari, H. K., Cox, B. J., Simmonds, A. J., Krause, H. M., Lipshitz, H. D., and Smibert, C. A. (2007) A multiprotein complex that mediates translational enhancement in Drosophila. *J. Biol. Chem*. **282,** 34031–34038
121. Kwon, S., Barbarese, E., and Carson, J. H. (1999) The cis-acting RNA trafficking signal from myelin basic protein mRNA and its cognate trans-acting ligand hnRNP A2 enhance cap-dependent translation. *J. Cell Biol*. **147,** 247–256
122. Kosturko, L. D., Maggipinto, M. J., Korza, G., Lee, J. W., Carson, J. H., and Barbarese, E. (2006) Heterogeneous nuclear ribonucleoprotein (hnRNP) E1 binds to hnRNP A2 and inhibits translation of A2 response element mRNAs. *Mol. Biol. Cell* **17,** 3521–3533
123. Ponting, C. P. (2000) Novel eIF4G domain homologues linking mRNA translation with nonsense-mediated mRNA decay. *Trends Biochem. Sci*. **25,** 423–426
124. Mazza, C., Ohno, M., Segref, A., Mattaj, I. W., and Cusack, S. (2001) Crystal structure of the human nuclear cap binding complex. *Mol. Cell*. **8,** 383–396
125. Hosoda, N., Kim, Y. K., Lejeune, F., and Maquat, L. E. (2005) CBP80 promotes interaction of Upf1 with Upf2 during nonsense-mediated mRNA decay in mammalian cells. *Nat. Struct. Mol. Biol*. **12,** 893–901
126. Kim, K. M., Cho, H., Choi, K., Kim, J., Kim, B.-W., Ko, Y.-G., Jang, S. K., and Kim, Y. K. (2009) A new MIF4G domain-containing protein, CTIF, directs nuclear cap-binding protein CBP80/20-dependent translation. *Genes Dev*. **23,** 2033–2045
127. Nakamura, A., Amikura, R., Hanyu, K., and Kobayashi, S. (2001) Me31B silences translation of oocyte-localizing RNAs through the formation of cytoplasmic RNP complex during Drosophila oogenesis. *Development* **128,** 3233–3242
128. Johnstone, O., Deuring, R., Bock, R., Linder, P., Fuller, M. T., and Lasko, P. (2005) Belle is a Drosophila DEAD-box protein required for viability and in the germ line. *Dev. Biol*. **277,** 92–101
129. Meignin, C., and Davis, I. (2008) UAP56 RNA helicase is required for axis specification and cytoplasmic mRNA localization in Drosophila. *Dev. Biol*. **315,** 89–98
130. Cauchi, R. J. (2012) Conserved requirement for DEAD-box RNA helicase Gemin3 in Drosophila oogenesis. *BMC Res. Notes*. **5,** 120
131. Surabhi, S., Tripathi, B. K., Maurya, B., Bhaskar, P. K., Mukherjee, A., and Mutsuddi, M. (2015) Regulation of Notch signaling by an evolutionary conserved DEAD Box RNA helicase, Maheshvara in Drosophila melanogaster. *Genetics* **201,** 1071–1085
132. Wang, Z. A., Huang, J., and Kalderon, D. (2012) Drosophila follicle stem cells are regulated by proliferation and niche adhesion as well as mitochondria and ROS. *Nat. Commun*. **3,** 769